Development of Nanosensor to Detect Mercury and Volatile Organic Vapors

by

Chang Heng Yang

Department of Civil and Environmental Engineering
Duke University

Date: 07/22/2010
Approved:

_____
Marc Deshusses, Supervisor

_____
Heileen Hsu-Kim

_____
Zbigniew J. Kabala

Thesis submitted in partial fulfillment of
the requirements for the degree of Master of Science in the Department of
Civil and Environmental Engineering in the Graduate School
of Duke University

2010

ABSTRACT

Development of Nanosensor to Detect Mercury and Volatile Organic Vapors

by

Chang Heng Yang

Department of Civil and Environmental Engineering
Duke University

Date: 07/22/2010
Approved:

_____
Marc Deshusses, Supervisor

_____
Heileen Hsu-Kim

_____
Zbigniew J. Kabala

An abstract of a thesis submitted in partial
fulfillment of the requirements for the degree
of Master of Science in the Department of
Civil and Environmental Engineering in the Graduate School
of Duke University

2010

Abstract

The properties of nanoparticle sensors intended for real- time monitoring of low concentration of elemental mercury (Hg) vapor and volatile organic compounds (VOCs) are presented and discussed. Nanosensors made of conducting polypyrrole (PPY) and tin dioxide (SnO_2) on SWNTs were tested for the detection of volatile organics such as benzene, methyl ethyl ketone (MEK), hexane and xylene. The greater sensitivity of these two sensors to lower analytes concentrations compared to previous research studies was demonstrated. Experiments were conducted at room temperature, and the response was shown to be fast and highly sensitive to low concentration of VOCs. An attempt of using PPY and SnO_2 sensors in a sensor array to quantify MEK and benzene in a mixture partially failed, as it was not successful in accurately quantify both compounds in a mixture. Sensing mechanisms of these two sensors to analytes are discussed in this thesis.

Experiments were conducted with similar nanosensors for sensing elemental mercury vapors. This sensor for mercury vapors is composed of gold (Au) nanoparticles on single-walled carbon nanotubes (SWNTs) networks. Surface topography was determined by scanning electron microscopy (SEM). The electrical resistance of Au-SWNTs networks drastically increased upon exposure to mercury vapor. The experiment result shows that higher deposition amounts of Au nanoparticles on SWNTs

lead to higher sensing responses. A detection limit of this senor to vapor mercury concentrations in the parts-per billion (ppb) was seen. Response features of current mercury sensors are discussed concerning sensitivity, reproducibility and regeneration at room temperature (25°C).

Further work to improve the sensors that were tested was identified. The main challenge of this sensor is that the response and regeneration time is relatively slow at room temperature, especially for Au nanoparticle sensors. Also, with respect to PPY and SnO_2 nanosensors, a high reproducibility in the making of sensors is desired. This improvement can help PPY and SnO_2 sensors to have better consistency. Finally, since nanosensors that can detect VOCs are not very specific, array sensing and numerical methods that can be used to quantify individual compounds in mixtures using nanosensors array data are needed.

Contents

List of Tables

List of Figures

Acknowledgements

I would like to express my sincere gratitude to my advisor--Dr Deshusses. His industrious attitude to do research work and valuable recommendations on my research has instructed me greatly. Without his supervision, it is impossible for me to finish my research work and compose this thesis.

I would like to thank Dr. McNicholas for giving me valuable instructions on the improvement of experimental methods and appropriate manners to make presentations. I would also like to thank Dr. Hsu-Kim and Dr. Kabala for their opinions on my thesis.

Last but not least, I would like to thank God, all my family, my friends and my girl friend, Siyao Zhang for their continuous support on my research. Their prayer, care and encouragement enabled me to finish my research and enjoy an interesting life in the United States.

1. Background

In recent decades, there has been an increasing demand for various gas sensors devices to detect different gases or vapors for a large number of applications. Several gas sensors can be regarded as warning signals in our daily life. For example, semiconductor gas sensors coated with metal oxides serve as alarms as they are sensitive to flammable gases such as CH_4 and H_2 in domestic houses or industries. In the industry field, oxygen sensors also play an important role for car emission control as well as metallurgical process control. Humidity sensor functionalized polymers are capable of detecting water vapor for automating food processing and air conditioning. Other gases sensors also exhibit high sensitivity to toxic gases like H_2S and NH_3 can be useful in either industrial settings or agricultural applications. A growing demand exists for sensitive sensors in homeland security, health, and food security areas. These examples show the importance of gas sensor technology related to environmental monitoring and process control [1, 130].

1.1 Introduction to VOCs and sensors for VOCs

1.1.1 Source of Volatile Organic Compounds

VOCs emissions include natural processes and anthropogenic activities. Natural volatile organic compounds result from oceans, plant foliage, forest and animals [1]. Among them, VOCs emitted from animal facilities include a wide variety of VOCs, some of which presenting environmental health risks and/or odor nuisances. These VOCs

include acids, alcohols, aromatic compounds, etc. Frequently, odors from animal production facilities related to the storage and decomposition of manure. Manure odors are a complicated mixture of acids, aromatic compounds, heterocycles and amides [1]. Anthropogenic sources of VOCs include vehicles emission, industries using volatile solvents, industrial sources [1, 2]. Research has also shown that traces of VOCs are the main indoor air pollutant, usually released from building materials. The VOCs are emitted from these materials by several mechanisms such as oxidation, decomposition, and desorption processes [3]. Although they exist at very low concentrations (ppb or lower), these VOCs can cause adverse effects to human. These effects include nose and throat discomfort, nausea, dizziness and headache [1]. Some VOCs such as benzene, toluene, and ethylbenzene, have been shown to be carcinogens to humans.

1.1.2 Toxicity and Regulation of Volatile Organic Compounds

Hazardous VOCs need to be regulated to decrease toxic effects to whoever is exposed to dangerous levels of these compounds. In an industrial environment, workers can be at high risk near vents and stacks, or during manipulation of the chemicals. Therefore, a series of limits are enforced to protect workers. For example, Occupational Safety & Health Administration (OSHA) sets permissible exposure limits (PEL) to keep workers away the adverse effects from toxicants. PEL are warning levels concentration of a specific substance in the air for occupational exposure [4]. For example, PEL for xylene is 100 ppm of air, which is a fairly high level, indicative of the fact that xylenes

will only cause moderate adverse health effects even at ppm levels. PEL for MEK, hexane and benzene are 200, 500 and 1 ppm, respectively, which illustrates the greater concern about benzene and its carcinogenicity. Regulations for VOCs emissions are complex, and depend on the compound and specific local, state or federal regulations.

1.1.3 Monitoring Methods of Volatile Organic Compounds

Volatile organics encompasses a very broad range of substances, which end in the environment as a result of natural processes and industrial and anthropogenic activities. For the purpose of this thesis, we will only be concerned with industrial and anthropogenic activities and low molecular weight VOCs. Such VOCs are mainly produced from anthropogenic activities such as painting production facilities, oil processing plant, metal and plastic foundries, etc. [4]. VOCs can be seen as hydrocarbon compounds with a boiling point below 200 °C and higher vapor pressure and often a low water solubility; moreover, they can exist in atmosphere, soil, ground water and surface water [6, 7]. The U.S. Environmental Protection Agency (EPA) has shown that carcinogenic nature of VOCs can cause adverse human health effects in the indoor environment, which aggravate illness such as asthma, allergies and cancer [6-10]. Studies have shown that principal toxicants that draw people's attention include some VOCs, such as benzene, toluene, acetone, xylene and ethylbenzene [5, 7]. The requirement of high-performance sensors is needed to monitor and detect these gas species at ambient temperature. Gas analyzers like gas chromatography (GC) and mass

spectrometry (MS) can help quantify and detect these gas samples. However, they are expensive and convenient for use only in the laboratory [7, 11, 12]. Existing methods should allow an easy monitoring and be stable in various environments [11]. Some sensors that exist include devices based on bulk materials such as metal oxides (SnO_2) [12-16] and conducting polymers (PPY) [5, 10, 13, 17-19].

Typical concentrations of interest for monitoring VOCs vary broadly:

- Ultra low trace concentrations (ppt or lower) for ambient monitoring.
- Low concentrations (roughly 1 ppb to 1 ppm) for some ambient air studies, personal exposure or trace emissions.
- Low ppm to tens or hundreds of ppm, for most industrial emissions, and some chemical alarms.
- High concentrations (hundreds of ppm) for industrial exhausts, concentrated emissions, spill response, high level chemical alarms.

1.1.4 SnO_2 film Sensors

Probably the most used VOC gas sensor is the SnO_2 film sensor, which has been shown to be broadly sensitive to various groups of analytes including VOCs and greenhouse gases [20-22]. Research studies have shown that SnO_2 sensors display high sensitivity to polar analytes. Researchers hypothesized that polar compounds are adsorbed to a greater extent on the surface of SnO_2 than non-polar compounds [20]. Much effort focused on developing SnO_2 gas sensors including thin film sensors and

semiconductor gas sensors sensitive to VOCs like xylene, methanol, methyl ethyl ketone (MEK), benzene and hexane. These sensors usually have detection limits in the ppm range. However, the main drawback of SnO_2 film sensors is their needed to operate at higher temperature (between 200°C and 500°C) and their lack of specificity in distinguishing different VOCs [13, 20].

1.1.5 Conducting Polymer Film Sensors

Conducting polymers (CPs) such as PPY, polyaniline (PANI), oxyacetylene (PAC) and polythiophene (PTH) have attracted a lot of research interest as they are promising sensing material with interesting tunable electrical properties [10, 13, 23]. Among these conducting polymers, PPY has been considered as a good candidate for high electrical conductivity, room temperature operation and real-time monitoring sensors [24]. PPY sensors have mainly been used to detect NH_3 and show high sensitivity at room temperature [5, 10, 25, 26]. Analytes may have physical interaction with PPY which then changes the electrical conductivity directly because of adsorption of the analyte or indirectly via swelling and morphological changes [5, 13, 27]. For example, NH_3 molecular adsorption into PPY polymer films may lead to a repulsive force between PPY chains resulting in a swelling of PPY films. This swelling may reduce holes in the PPY and increase the resistance of the resistance of the film [11, 13, 25, 27]. PPY film and PPY composite sensors are shown to be sensitive to VOCs like benzene, xylene, ethylbenzene and toluene. The response behavior of PPY film sensor with 40 minutes exposure to

these vapors (above 50 ppm) was presented [5]; moreover, the response time for PPY composite sensors ranged from 3 to 8 minutes when exposed to more than 100 ppm [7, 10, 23]

1.2 Source of Mercury

Global mercury emissions have been an increasing concern over the past century; they are stemming from natural sources and anthropogenic sources [29-33].

The natural emissions of mercury come from land and water-body surface; however, the natural content of mercury varies highly because of unstable environmental situations [30, 34]. The mercury emitted from volcanogenic source, evaporation from land and water body surfaces, burning of crop residue and forest fires [30, 31, 35-37]. In these cases, the main form of mercury is elemental mercury. Mercury emission from surface waters pertains to main natural resources. Current studies show that the evasion of mercury vapor is caused by the difference in temperature and mercury concentration at the air/water interface. In addition, the UV radiation present in sunlight has also been shown to help increase the mercury emission [31, 38-40]. Overall, mercury emission from lakes and oceans surface dominates the natural sources, followed by the biomass burning and volcanogenic sources. They have been estimated to range from 500 to 5000 tons per year [30, 31].

Mercury emissions from industrial use is the main source released to the atmosphere, including coal-fired electric utilities and municipal waste incineration [32-

34, 41-44, 45], caustic soda production [31, 33, 41, 46, 45], non-ferrous metals manufacturing facilities [31, 33, 47, 45], and cement plants [31, 33, 41, 45, 48]. Mercury emission from coal and fire combustion is the major anthropogenic source in the world with an estimated release of 810 tons per year [31, 32, 41, 42, 44, 49]. Recently, China has been the largest coal energy consumption country, around 213.8~268.0 Mg yr^{-1} over the past twenty years [31, 41, 50]. Researchers suggest that coal energy has been the dominant power supply in China's domestic energy consumption; In addition, limited dust control devices in coal-fired power facilities in also increases the mercury emission to the atmosphere [33, 41]. Intensive anthropogenic sources have released a huge amount of mercury to the atmosphere for decades [29, 31, 32, 34].

1.3 Transport of Mercury

As seen in figure 1, the mercury emissions released from anthropogenic and natural sources undergo chemical and physical reactions. Figure 1 shows schematic of mercury emissions from combustion and natural sources as well as describes the mercury transport in the atmosphere and aqueous system [32].

Mercury is released into atmosphere from coal-fire facilities and waste incineration plus natural sources such as forest fire and volcanic eruptions in figure 1. Elemental Mercury (Hg^0) released from these sources [31-33, 41] was shown to stay in the atmosphere for 0.5-2.0 years because of a high vapor pressure and low water solubility [32, 34, 51, 52]. Hg^0 undergoes oxidation and dry as well as wet deposition [32,

53-56]. Due to the existence of strong oxidizing agents such as hydrogen peroxide (H_2O_2) and ozone (O_3), the Hg^0 is oxidized to divalent mercury (Hg (II)) at pH<7 [32, 55, 56]; moreover, chlorine (Cl_2) in coal [32, 57] also reacts with Hg^0 to form Hg (II) as Hg^0 has been shown to be the fast reaction between these two compounds [32, 58]. Dry deposition including fallout and interception may be an important factor to precipitate airborne Hg^0 passing over trees canopies [32, 59]; in addition, water-soluble Hg (II) may tend to be removed by wet deposition including rainwater and excess water from leaves to the ground [32, 59, 60], or be reduced to Hg^0 in the presence of sulfite (SO_3^{2-}) [32, 61].

Recent attention has drawn to the transport of mercury in aquatic system due to the existence of highly toxic methylmercury (MeHg) [62-66] in figure 1. Hg (II) may be formed when Hg^0 from point source pollution [32, 34, 64] or the evaporation from the surface of water bodies [31, 37], undergoes oxidation due the O_3 or other photogenerated oxidants. Sulfate-reducing bacteria play an important role in transforming Hg (II) into MeHg in anaerobic sediments [62, 67-72]. MeHg is the main bioaccumulative mercury species that is taken up by biota and accumulates in fish [42, 73-75]. Consumption of Hg-containing fish has been linked to high MeHg concentrations in the human body like blood [42, 76].

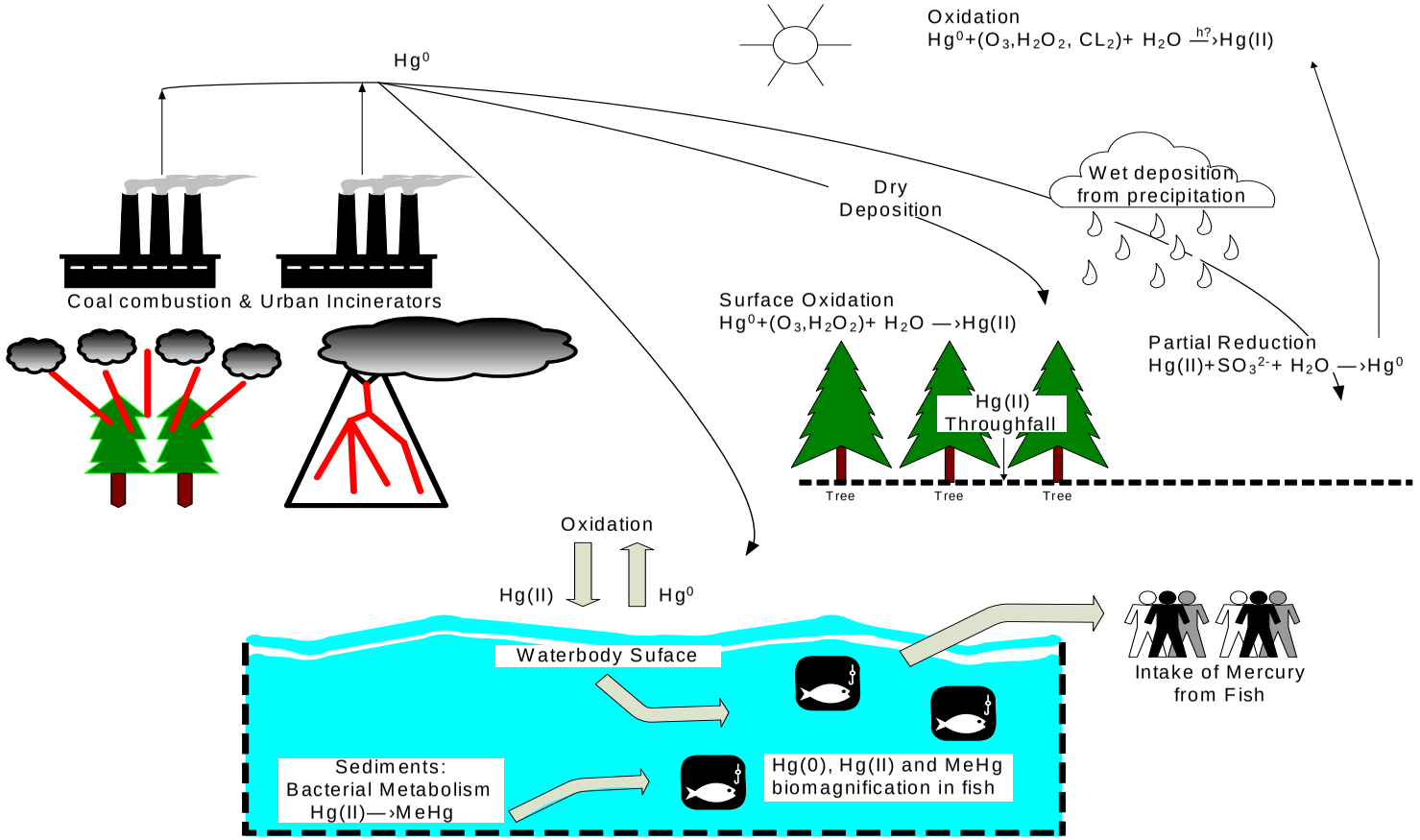

Figure 1: Brief introduction of natural and anthropogenic mercury transport in the atmosphere and waterbodies (Modified from [4, 9])

1.4 Toxicity Effects of Mercury on Human

Numerous researchers in recent years have investigated the toxicity of mercury on the human body. Mercury exists in three chemical forms, elemental form (Hg^0), the divalent inorganic form (Hg (II)) and organic compounds, mostly as MeHg. MeHg has been shown to be especially toxic to human health by animal experiments and previous events.

Hg^0 poisoning has been observed after exposure to Hg^0 vapors for example in occupational labor [77-83]. Inhalation of Hg^0 vapors exceeding 500 $\mu g/m^3$ may cause toxicity to central nervous system (CNS), inducing numerous symptoms like loss of memory, fever, malaise, cough and neurocognitive disorders [29, 42, 77, 84]. In addition, several medical documents also show infants who inhale of high concentration of Hg^0 may develop lung disorder [85-87]. Main pathway of Hg^0 exposure in children includes exposure to mercury dust and powder by either crawling on the floor or accidently ingesting objects such as thermometers [29, 88, 89].

Hg (II) is found in the human body through the oxidation of Hg^0 binding with red blood cells in the lungs [29, 90]. Accumulation of Hg (II) in kidneys is higher than that in brain and liver [29, 91]. Moreover, low μM concentration of Hg (II), which showed strong thiol-binding activity, blocks DNA binding as well as cause cell death [42, 92]. For example, chloralkali workers exposed to mercury have been demonstrated to have impaired kidney functions [42, 93].

MeHg is the most toxic mercury form and easily absorbed into body tissues [77, 94]. In addition, MeHg is prone to accumulate in aquatic living organisms and has been shown to accumulate to high concentration in specific species of fish [42, 76, 95-98]. Those who consume large amounts of these fish are at high risk to MeHg poisoning [42, 77]. Previous accidental events and animal experiments have revealed that significant response of MeHg intake induced central nervous system toxicity, caused by MeHg transport across the blood b-brain barrier and disrupting the brain function [77]. For instance, animals tests have shown that MeHg was found in the rat's brain after injection [29, 99-101]. In addition, MeHg can cause severe damage to the developing brain, resulting in decreased activity of cell and neuron [102-104]. Hg chronic exposure is an increasing problem in modern societies, and has been considered as a serious problem. But for this to be solved, reliable and fast monitoring methods that can detect low concentrations of mercury are needed.

1.5 Sensors for Detection of Mercury Vapor

In the past decade, one has seen an explosion of interest in sensors to detect all kinds of air pollutants, including mercury vapor. Research has shown that metallic gold films are highly sensitive to vapor mercury vapor, produced an increased resistance upon exposure to mercury vapor due to the formation of an amalgam [105-107]**.** Currently available sensors for monitoring mercury vapor include surface acoustic

wave-based sensor (SAW-based sensor) [106, 108], piezoelectric sensor [108, 109], nanosensors [44, 107, 108-111], and polymer-carbon composite sensor [107, 112, 113].

Desirable features for gas sensors include low energy and material consumption, high sensitivity and specificity to various analytes, regeneration or reversibility at room temperature, commercially available materials and simple manufacturing using existing techniques, low cost, stable quality in different environments, and continuous monitoring of analytes for mobile applications [44, 107, 113]. In the next sections, selected mercury sensors are reviewed.

1.5.1 Surface Acoustic Wave-Based and Piezoelectric Sensors

Surface Acoustic Wave (SAW)-based sensors provide high sensitivity to mercury vapor [106, 108, 114]. This sensor is mainly composed of a high frequency acoustic dual delay line oscillator and an angstrom thin gold sensing film deposited on one delay path. The other delay line can represent as a reference to diminish environmental effects such as humidity and temperature vacillation. The amalgamation due to the exposure to mercury causes a different frequency between the sensing and reference delay line oscillators. The concentration of mercury vapor can be determined according to the difference of oscillation frequency. In addition, SAW-based sensors offer high sensitivity of detecting vapor mercury at parts-per-million (ppm) and parts-per-billion (ppb) levels [107, 108]. The sensing mechanism of piezoelectric sensors is based on the lower vibration frequency of thin quartz plate coated with metallic gold films on both sides

within the actual sensor. Good responses of this sensor to mercury vapor levels in the ppm range was been presented [108, 109]. The disadvantages of these two sensors are that they show sensitivity to mercury vapor over a limited temperature range and that regeneration can only be completed at high temperature (i.e., 200°C) [106, 109]

1.5.2 Gold Film / Nano-Wire Sensors

Recently, there has been an increase in studies of ultrasensitive sensors based on nanoscale materials. Often, these nanosensors provided enhanced sensitivity toward the analytes, less energy-consumption, and could be developed in small portable devices for continuous on-site monitors [115, 116]. Recently, NASA has shown the interest in sensors to detect mercury vapor inside spacecrafts for when mercury would be released from a broken light. Sensors to detect concentration as low as ppb Hg concentrations are required to monitor astronauts' health [107, 117]. For example, gold film sensors have been proven to be standard applications used in laboratory and commercial instrument. The abraded gold films are prepared in vacuum, with high speed abrasive particles thinning and roughening films. Gold films are made around 15 nm thick and show pronounced sensitivity to mercury vapor in the ppb range at room temperature. However, gold film sensors regeneration can only be achieved at high temperature up to 200°C [105, 107, 118, 119]. The intense interest in nanowire sensors has been shown in scientific research such as biosensors [115, 120]. The gold nanowires were fabricated with the e-beam lithography/ lift-off process or template electrodeposition. Nanowire

sensors also show significant sensitivity to mercury vapor because of nanoscale properties including elevated surface area to volume ratio (SAVR). A recent research paper showed that nanowire sensors are competitive with existing gold film sensors upon exposure to mercury [44]. The nanowire sensors' detection limits are at low concentrations of 5 ppb. However, the main drawback of nanowire sensor can not be regenerated after use [110].

1.5.3 Polymer-Carbon Composite Sensors

Sensor arrays composed of polymer-carbon composite films have been broadly responsive to low concentration of volatile organic compounds (VOCs) and showed that arrays can detect and distinguish various gas analytes. Polymer mixtures combined carbon black, the stable and conductive element, with organic polymers that provide various chemical properties have been proven to be quite stable under a long-term use [121, 122]. Gold films on polymer-carbon composite films have been proposed for mercury sensing. They are composed of polymer films deposited with 10 nm thick gold films [107]. Mercury will amalgamate gold, which either spread on or penetrate beyond polymer-carbon composite films. Amalgamation formed both on and through composite films influences the conductivity. In addition, composite polymer films can also respond to different organic vapors. Research has shown that this composite mercury sensor can detect 10 ppb levels of mercury vapor and can regenerate adequately at moderate temperature for use [107].

1.6 Introduction to gas nanoparticle sensors

Novel nanosensors based on functionalized SWNTs were developed jointly by the research groups of Dr. Nosang V. Myung at University of California Riverside (UCR) and Dr. Marc Deshusses, when still at UCR. The sensors are based on functional nanoscale materials possessing unique properties such as higher surface area accessible for sorption and reaction [123, 124]. The functionalization technology that was selected is electrodeposition, which provides easy fabrication, cheap and powerful way of decorating nanoscale sensing materials onto materials such as SWNTs [125]. The research work in my thesis includes two parts. The first part is concerned with the use arrays of gold, conducting polymer and SnO_2 functionalized SWNT sensors in an attempt to detect low concentrations of VOCs. Both sensing of individual analytes and of mixtures is attempted. The second part deals with the results of my assistance with mercury sensing experiments done by Dr. Thomas McNicholas. These experiments are the first attempt to use SWNTs decorated with gold nanoparticles to test the sensing sensitivity of mercury. It is my hope that my thesis can be helpful for researchers who are focusing on the development of nanosensors for low concentrations of toxic gases and vapors.

2. Objectives and hypothesis

2.1 Objectives

The goal of my research is firstly to provide data on individual VOC sensing and mixture of VOCs sensing using sensor arrays that include bare SWNT, Au, PPY and SnO_2 nanoparticles deposited on SWNTs. A second objective is to discuss the response characteristics of novel mercury vapor nanosensors. Several aims discussed in this thesis include the investigation on feasibility to use nanosensors arrays to quantify and discriminate various VOCs, the relationship between deposition charge of Au nanoparticles and sensitivity, the characteristics of the sensors. Hopefully, this sensor arrays functionalized with PPY, SnO_2 and Au can be developed later as wearable sensors to detect vehicle exhaust and serve as indoor air quality monitoring device.

2.2 Hypothesis

My research is based on the hypothesis for the VOCs experiments is that each VOC or VOC mixture will be generating different sensing responses on sensor arrays made of SWNTs with functional groups such as Au, PPY and SnO_2. Furthermore, the hypothesis is that the resistance changes will result from the reaction of mercury and Au nanoparticles on SWNTs networks and that these Au nanoparticle sensors will provide high sensitivity, reproducibility and reversible properties compared to current mercury sensors.

3. Materials and methods

3.1 Materials and Methods

3.1.1 Fabrication of functionalized SWNT sensors

The synthesis method is shown in figure 2. For this research, the sensors and sensor arrays were made by several researchers in the group instructed by Dr. Nosang V. Myung at UCR. The electrodes for the sensors were microfabricated on silicon substrate using standard lithographic patterning. Using chemical vapor deposition (CVD), one micron thick SiO_2 film was first deposited on a (100) oriented silicon wafer to insulate the substrate. After photo lithographically defining the electrodes, a Cr adhesion layer and a ~3000 Å-thick Au layer were e-beam evaporated. Finally, the electrodes were defined using lift-off techniques. The gap distance between electrodes was fixed at 3 μm.

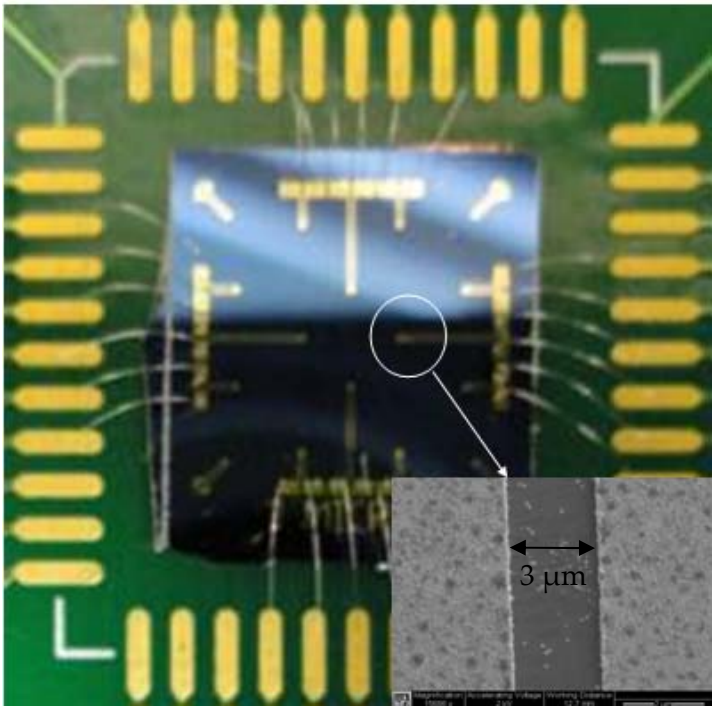

Figure 2: Optical picture of sensor array on chip carrier and SEM image of SWNT network across microfabricated gold electrodes (SEM acquired by Dr. McNicholas)

The fabrication steps of the Au nanoparticles decorated SWNTs are shown in Figure 3. Sensors Purified SWNTs-COOH, 80-90% purity, produced by Carbon Solution, Inc. Riverside, were dispersed across micofabricated gold interdigitated gold electrodes by positioning a 500 nL drop of aqueous solution with soluble SWNTs (1μg/ml) onto the interdigitated electrodes and allowing it to air dry to form an SWNT network bridging the electrodes. After formation of the SWNT network, some sensors were annealed at 300 °C for 30 minutes in an inert environment (i.e. 5% hydrogen and 95% N_2) to minimize the contact resistance between the CNT network and the gold pads.

Electrodeposition of gold nanoparticles on the SWNT networks was performed using three electrode electrochemical cell configurations. Commercially, available ready-to-use gold electroplating solution from Technic INC. (Techni-gold 25 ES, CA) was used as electrolyte. For gas studies, first, a 3 μL droplet of Au electrolyte solution was placed on top the SWNT network bridging electrode gap. Au alkaline cyanidefree gold electrolyte (pH=7.5) was selected to prevent the dissolution of a Cr adhesion layer which can be readily attacked in an acidic environment. Next, platinum and Ag/AgCl wires were positioned inside the droplets using a micropositioner. The annealed SWNT networks along with the gold electrodes served as the working electrodes, while platinum and Ag/AgCl wires served as the counter and pseudo reference electrodes, respectively. All depositions were carried out in a potentiostatic mode (constant potential) at 25 °C and ambient pressure, with deposition charge as the stopping criteria. After deposition, the electrodes were rinsed with deionized water and acetone to remove any metal salt residues and impurities [126].

The electrochemical studies for coating tin oxide on SWNTs was carried out using two electrolyte solutions. First 100 mM of $NaNO_3$ (≥99.0 %, Sigma-Aldrich, MO) is added to 75 mM of HNO_3 (70%, Sigma-Aldrich, MO) under constant stirring. 20 mM of $SnCl_2.5H_2O$ (≥98%, Sigma-Aldrich, MO) was then added, and the solution (pH ~ 1.3) was aged for 12 hours under constant stirring prior to use. Solution B was prepared using 20 mM of $SnCl_2.5H_2O$ in the absence of nitrate. The pH of the solution was adjusted to 1.3

using HCl (37%, Sigma-Aldrich, MO), and the solution was aged for the same amount of time. The electrodes were then immersed in the precursor solution and electrochemical studies were carried under quiescent conditions. SWNTs which were AC di-electrophoretically aligned between two gold electrodes separated by a 3 μm gap, served as the working electrode. Linear sweep voltammetry (LSV) and chronoamperometry measurements were carried out at room temperature for both device configurations in a three electrode electrochemical setup using a commercial potentiostat/galvanostat (EG&G, Princeton Applied Research 263A Potentiostat / Galvanostat, NY) with Pt wire (99.99%, Sigma-Aldrich, MO) and chlorinated Ag/AgCl wire (home made) as auxiliary and reference electrodes. An electrochemical cell was formed by dispensing a 3 μL drop of electrolyte solution on top of the aligned SWNT network and platinum and Ag/AgCl wires were positioned inside the droplet using micropositioner. For time dependent studies, a suitable cathodic potential (-0.4 V vs. Satd. Ag/AgCl for solution A and -0.6 V vs. Satd. Ag/AgCl for solution B) was applied for a defined period of time. It should be noted that after deposition, the working electrodes were immediately rinsed with water in order to prevent any undesirable residues and chemical precipitation. A control experiment was carried out in the same conditions for both the solutions but with no applied potential, to confirm the absence of any undesirable side reactions or chemical precipitation happening on the substrate [127].

The electrochemically functionalized PPY-AWNT based sensor was fabricated as follows: First, interdigitated gold electrodes with a 5 μm gap were microfabricated in-house using standard lithography. Using chemical vapor deposition, one micron thick SiO_2 film was deposition on a (100) oriented silicon wafer to insulate the substrate. After photolithographically defining the electrode area, a Cr adhesion layer and a ca. 3000 Å-thick Au layer were e-beam evaporated. Finally, the interdigitated gold electrodes were defined using lift-off techniques. Next, SWNTS (SWNT-COOH 80-90% purity. Produced by Carbon solution, Inc. Riverside) were dispensed across microfabricated gold interdigitated gold electrodes by positioning across microfabricated gold interdigitated gold electrodes by positioning 0.5 μL drop of aqueous solution with soluble SWNTs (1 μg/ml) onto the interdigitated gold electrodes and allowing it to air dry to form an SWNT network bridging the electrodes. After formation of the SWNT network, some sensors were annealed at 300 °C for 30 minutes in an inert environment (i.e. 99.999% argon) to improve the contact between SWNTs and electrodes. 5 μL of tetraethylorthosilicate (TEOS), 50 mL of ethyl alcohol (EtOH), and 1 mL of 1M HCl were mixed for 5 minutes and left to sit for 1 hour to stabilize. Two different methods were used for electropolymerization of aniline on the SWNTs. The first consisted of a two-electrode configuration and application of 1.5 VDC for 5 minutes across selected

individual channels of the sensor chip to electropolymerize aniline. The second method, allowing more precise control over the electropolymerization, involved a three-electrode configuration in which the SWNT network on the interdigitated gold electrodes, a stainless steel tip, and a Ag/AgCl wire were used as the working, counter, and reference electrodes, respectively. The Polypyrrole was deposited on the SWNTs potentiostatically (constant potential mode) at 0.8 V vs. wire. The coating thickness of Polypyrrole was adjusted by controlling the deposition time [124, 128].

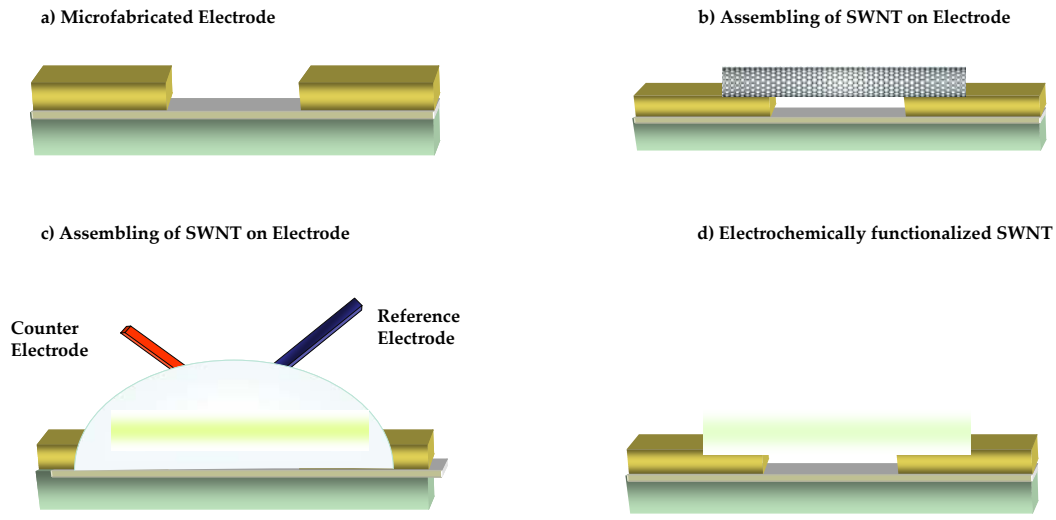

Figure 3: The fabrication of Au nanoparticle sensor. a): Preparation of electrode on silicon substrate; b) Assembling of nanotubes network between electrodes; c) of electrochemical functionlization of SWNTs; d) Deposited functional material (here shown as continuous film) onto the SWNTs (presentation figure from Dr. Deshusses)

3.1.2 Apparatus for the mercury and VOC sensing

The apparatus for the experimental set up used for the gas sensing is shown in Fig 4 and 5. A load resistance was selected to be as close as possible to the original resistance of the sensor to increase the accuracy of the measurements. A fixed voltage was applied to the circuit and the electrical resistance of the sensor was calculated from the value of the voltage over the load resistor and applying Ohm's law. The actual sensor test chamber was fitted with inlet and outlet tubes for gas flow-through over the sensor chip. Gas flow through the test chamber was controlled via mass flow controllers (Alicat Scientific Incorporated, Tucson, AZ). The air flow rate, set by a mass flow controller, was 200 cm^3min^{-1}. The electrical resistance of the load resistor was continuously monitored by using Fieldpoint analog input and output modules (National Instruments, Austin, TX) with a custom Labview program.

All experiments on Hg sensing were conducted by Dr. Thomas McNicholas in Dr. Deshusses laboratory. The sensors were first exposed to zero-grade air to achieve the baseline, then to a selected concentration of mercury gas. One test cycle was completed after the sensor's response reached a steady value. All experiments were conducted at room temperature [125, 126, 128].

All VOC sensing experiments were conducted by myself during the summer and fall of 2009. Analytes, such as benzene, hexane, MEK and xylene (purity of all compounds at least 99%), initially existing as a liquid phase were introduced in gas

sampling bag at appropriate amounts to produce the desired concentrations. The bags (figure. 5) were pressurized and the flow of VOC loaded air was regulated by mass flow controllers (Alicat Scientific Incorporated, Tucson, AZ) and diluted as needed with zero grade air. Zero-grade air was used to as a carrier gas and air flow rate was 200 cm^3min^{-1}. Electrical signals of VOCs sensors were continuously monitored and measured using Labquest (Vernier, Beaverton, OR) dataloggers. In all experiments, sensors were first exposed to zero grade air for at least 30 minutes to obtain the baseline, then to the selected concentrations of analytes until the response reached a steady value.

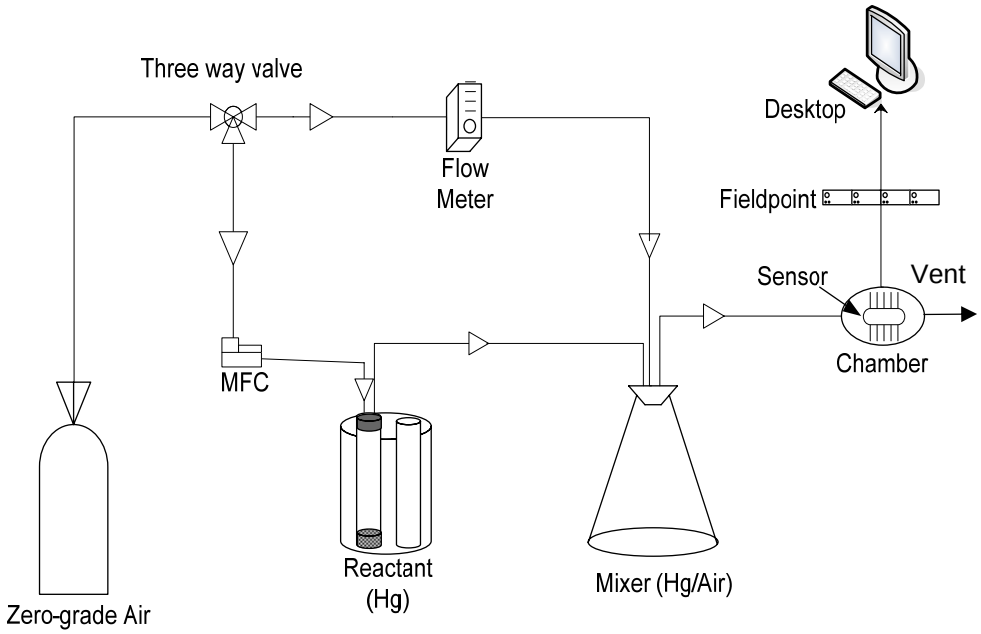

Figure 4: Schematic of mercury vapor sensing system

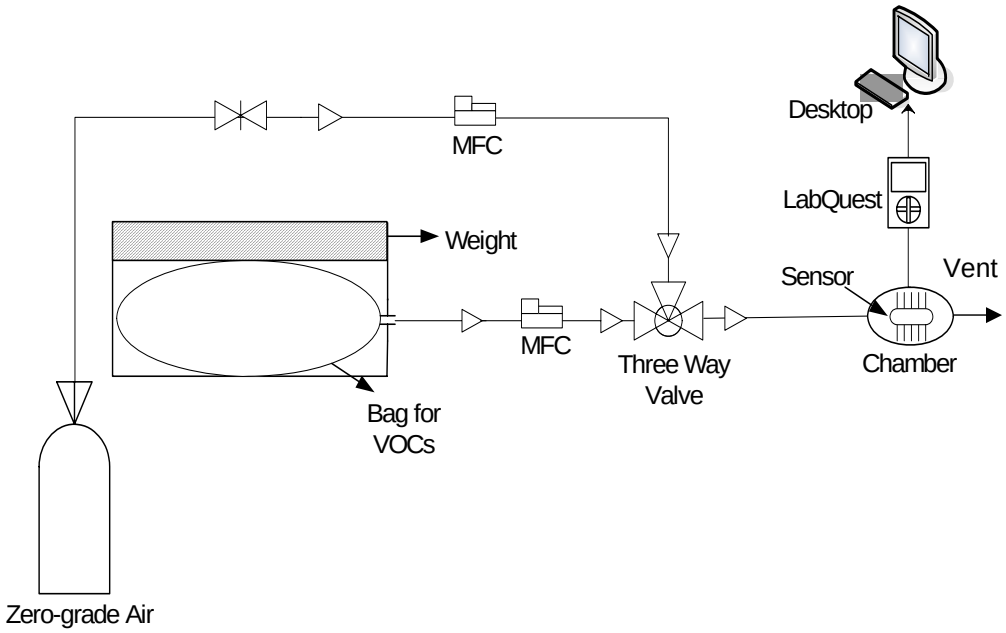

Figure 5: Schematic of VOCs vapor sensing system

4. Results and Discussion

4.1 Response characteristics of SnO_2 and PPY Functionalized SWNT to VOCs

4.1.1 Responses of SnO_2 and PPY SWNT sensors to VOCs

Sensing of benzene, MEK, hexane and xylene was conducted with PPY and SnO_2 decorated SWNTs. Typical real-time results are shown in Figure 6. In general, a relatively rapid response was observed after introducing the target VOC, with resistance changes observed as soon as within a few minutes. Steady state values were generally observed within 30 min. Similar to sensing of mercury vapor discussed later (see Section 4.3.2), self-regeneration of the sensors was observed at room temperature, although the recovery of the sensors was slower than the response after exposure to VOCs. The reasons for this were discussed by Strano [129] and are mainly due to the energy change in the adsorption process influenced by several mechanisms such as dipole-induced dipole interactions, the steric effects of nanoscale curvature, etc., although this remains partly speculative at this time.

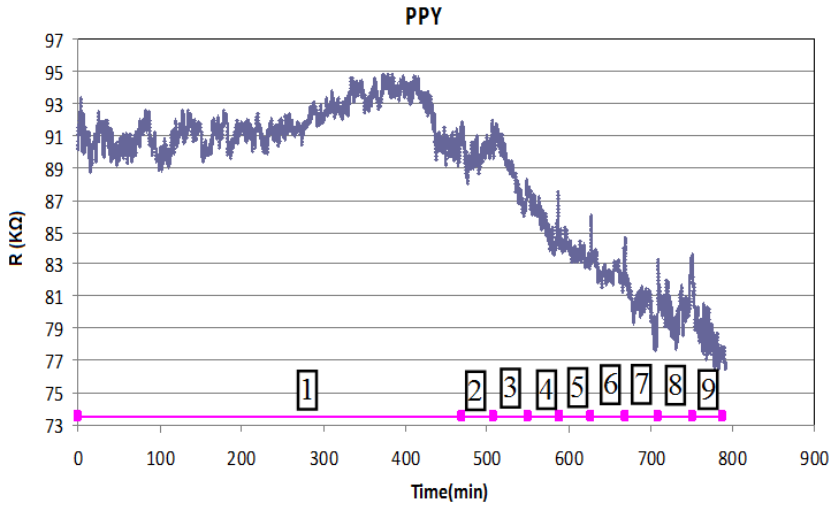

Figure 6: Real time response of the SWNT sensors functionalized with PPY to different concentrations of benzene and MEK. Concentrations of MEK for the different exposure phases were: 1) air purge, 2) benzene 13 ppm, 3) benzene 65 ppm, 4)MEK 13 ppm, 5) MEK 65ppm, 6)benzene 13 ppm and MEK 13 ppm 7) benzene 65 ppm and MEK 13 ppm, 8) benzene 13 ppm and MEK 65ppm, 9) benzene 65 ppm and MEK 65ppm

For VOCs sensing, the variability of measurements between experiment and between sensors was important. Variability between sensors was clearly the results on the manufacturing process by the researchers at UCR, where the sensors are produced. The making of the sensors is very prone to variations, e.g., drop placement during the position of the SWNT network, or differences in electrode placing during electrochemical functionalization. Variations within one experiment and drifts are more difficult to explain. Still, these drifts may lead to low reproducibility and low data quality. Errors between experiments may be from different factors. Different temperatures and humidity in the laboratory may cause variable responses. Also, after a series of experiments, the sensors may not function as well as usual, even after they are

baked in the vacuum oven for a long time. These interferences can exist if gases molecules interact with sensors surface so strongly that an irreversible chemical reaction or adsorption occurs. Some experimental uncertainties exist. The concentration of analytes may be affected by the bags for VOCs. These bags are repeatedly used for different VOCs and, although great care is used to prevent contamination, VOC residuals may exist in these bags by adsorption on bags surfaces even after purging with air for many times. Moreover, impurity in air may also influence the performance of gas sensors. Another variability of measurements may also be seen between the sensors. Same fabricated method will not produce two identical sensors. Different concentrations of substrates, densities of SWNTs between electrodes and thickness SiO_2 film would influence the response of same sensing material gas sensors. To address these issues, more experiments need to be conducted with replicate sensors. For example, duplicate experiments and controlled environment can help decrease the discrepancy caused by the environment and sensors themselves.

Figure 7 shows the nanosensors functionalized with SnO_2 exhibit broad responses to VOCs at low concentrations of benzene, MEK, hexane, and xylene. As it can be seen, SnO_2 sensors showed a higher sensitivity to MEK than to benzene, which is consistent with previous research [12, 14, 16, 20]. This result may be explained by the fact that MEK features a carbonyl group (C=O) as this group shows polar properties because of the electronegativity difference between the oxygen and carbon atoms.

Benzene is a non-polar molecular [23]. However, SnO_2 sensors exhibited higher sensitivity to hexane which is also non-polar. This result is not consistent with previous observations and hypothesis of polarity role. This would then indicate that polarity, if it plays a role, is not the only factor in generating a response on the nanosensors. Elucidation of the exact mechanisms would require extensive research with a variety of substances and possible development of structure-activity relationships.

Compared to previous researches, SnO_2 functionalized SWNT sensors show sensitivity to low concentration of VOCs at room temperature. Usual working temperatures for SnO_2 film sensors can be higher than 300°C, and even so higher concentrations of VOC are needed to observe significant signals in these studies [12, 14-16]. In summary, nanosensors with SnO_2 displayed excellent sensing properties towards VOC vapors.

Figure 8 reports the response of PPY-SWNT nanosensors upon exposure to various concentrations of four analytes; benzene, MEK, hexane, and xylene. Saturation was observed at MEK and benzene exceeding 13 ppm. It can be seen that PPY sensors exhibited higher sensitivity to MEK than benzene. Again, this could possibly be explained by the fact that ketones have a C=O bond, i.e., some polarity. This functional group may play a role altering the resistance of the sensors. This result is consistent with the research conducted by using nanowire PPY sensors [7]. In this research, it was shown that alcohol vapors, which all have hydroxyl functional group (O-H), can change

the resistance more than benzene type gases. Besides the greater sensitivity, the functionalized SWNT sensors showed a quicker response time than nanowire sensor. The previously reported nanowires sensor required more than 40 hours reaction time and had a sensitivity, which ranged from -0.15 % to -1.1%, to benzene with concentration ranging from 300 ppm to 1000 ppm [7]. With the current functionalized SWNT sensors, the sensitivity for benzene was higher than -2% for concentration of 13 ppm to 65ppm. It could be that our nanosensors have a greater functional group to surface area ration for VOCs adsorption and electrical resistance effect generation.

For xylene and hexane sensing, an increase in the resistance of the functionalized SWNT sensors to hexane and xylene vapors are observed (Figure 8 e and f). This result may be due to the swelling effect mentioned in the introduction. Nonpolar analytes may be adsorbed or absorbed into the PPY matrix, increasing the distance between PPY molecules and then lowering the conductivity. Earlier research also presented the same result in which increasing resistance for polymer sensors occurred upon exposure to nonpolar vapors [5, 13]. However, here, a decrease in the resistance of sensors to xylene and hexane vapors was observed in (Figure 8 d). The reasons for this and associated mechanism are still unclear [13].

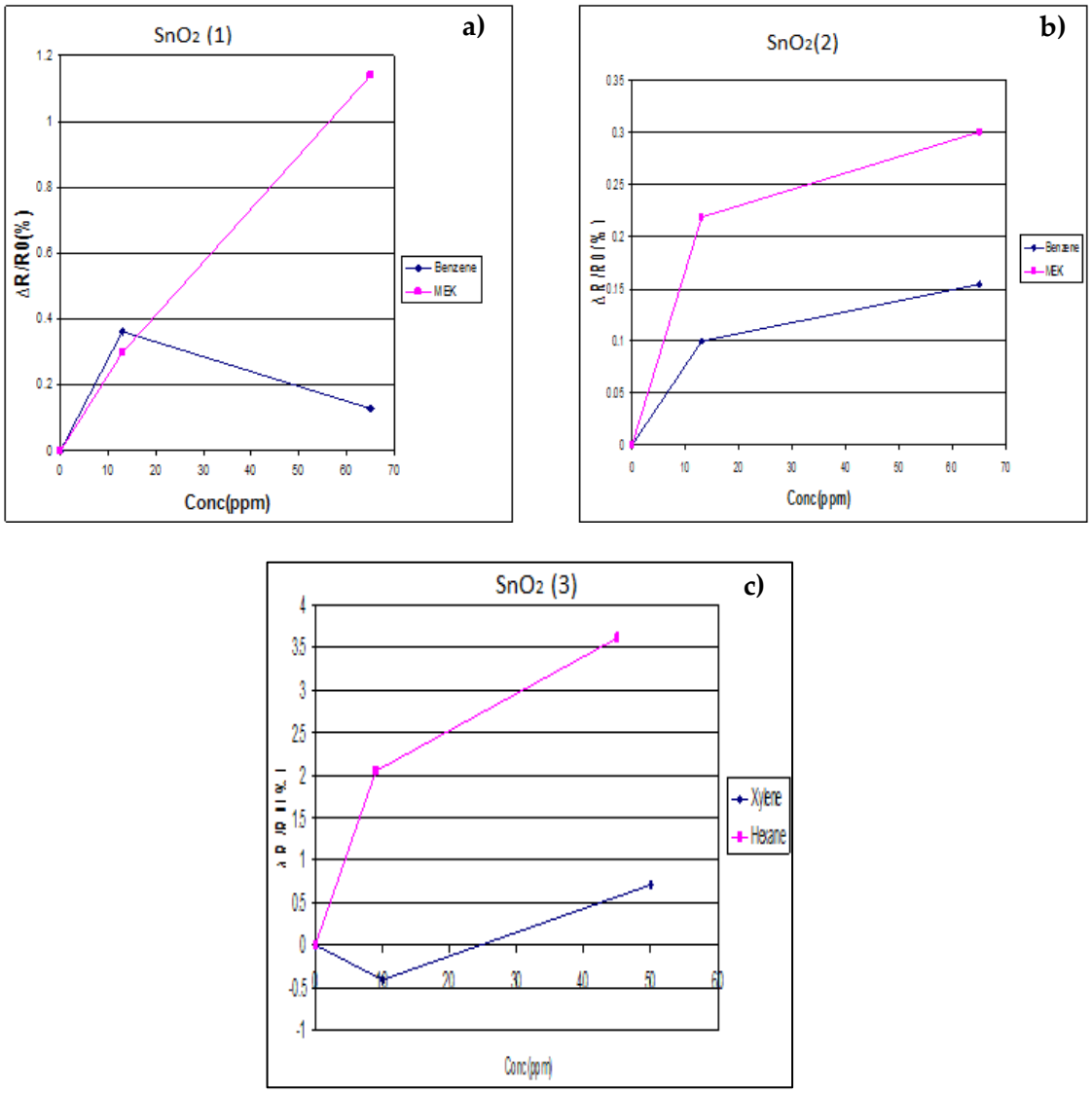

Figure 7: Response of two different SWNT nanosensors functionalized with SnO_2 to benzene and MEK (a, b); and one SnO_2-SWNT sensor to xylene and hexane(c)

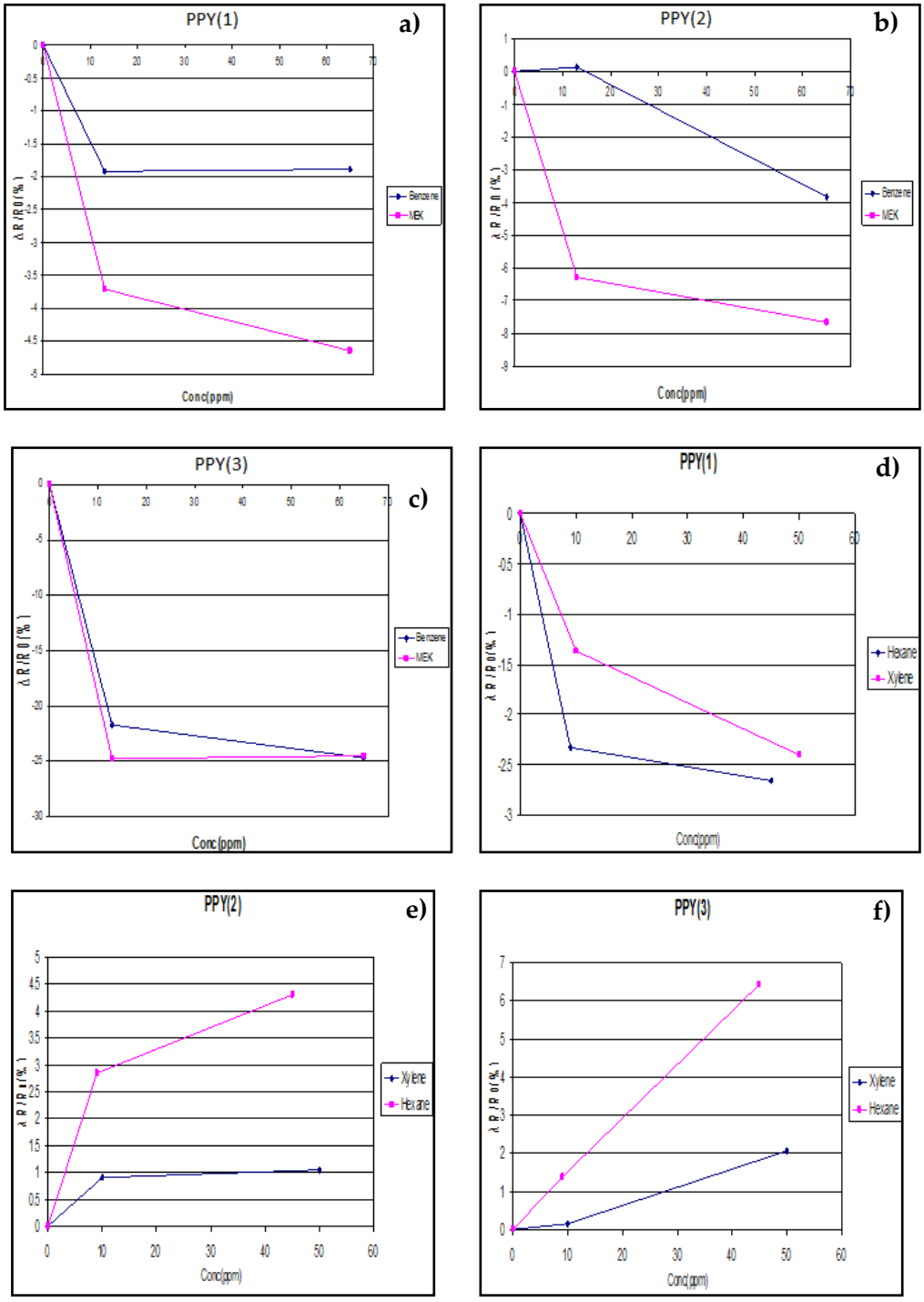

Figure8: Response of SWNT sensors functionalized with PPY to benzene and MEK (a-c); and xylene and hexane (d-f).

4.1.2 Response of a dual PPY and SnO_2 -SWNT array to a mixture of VOCs

Figure 9 shows that nanosensors made of SWNTs coated with PPY and SnO_2 exhibited different sensitivities to a mixture of MEK and benzene. The result displayed somewhat additive effects, especially obvious in Figure 9 b and d. This observation is consistent with the result mentioned above that PPY films exhibit higher affinity to MEK than benzene. This observation shows that PPY films show higher sensitivity to polar compounds and the resistance decreases after exposure to them. Besides, additive effects, increasing the resistance, observed when SnO_2 sensors exposed to a mixture of xylene and hexane may result from more molecules into films, lowering the conductivity. In brief, PPY sensors showed almost ten times higher sensitivity toward MEK and benzene than SnO_2 sensors. This may be relevant to distinguish between MEK and benzene with this particular sensor. According to previous research studies [16, 128], 10-fold difference in sensitivity is enough to distinguish between the target analytes. Thus sensors arrays that include different SnO_2 sensors may be differently sensitive to polar and nonpolar VOCs such as MEK and benzene.

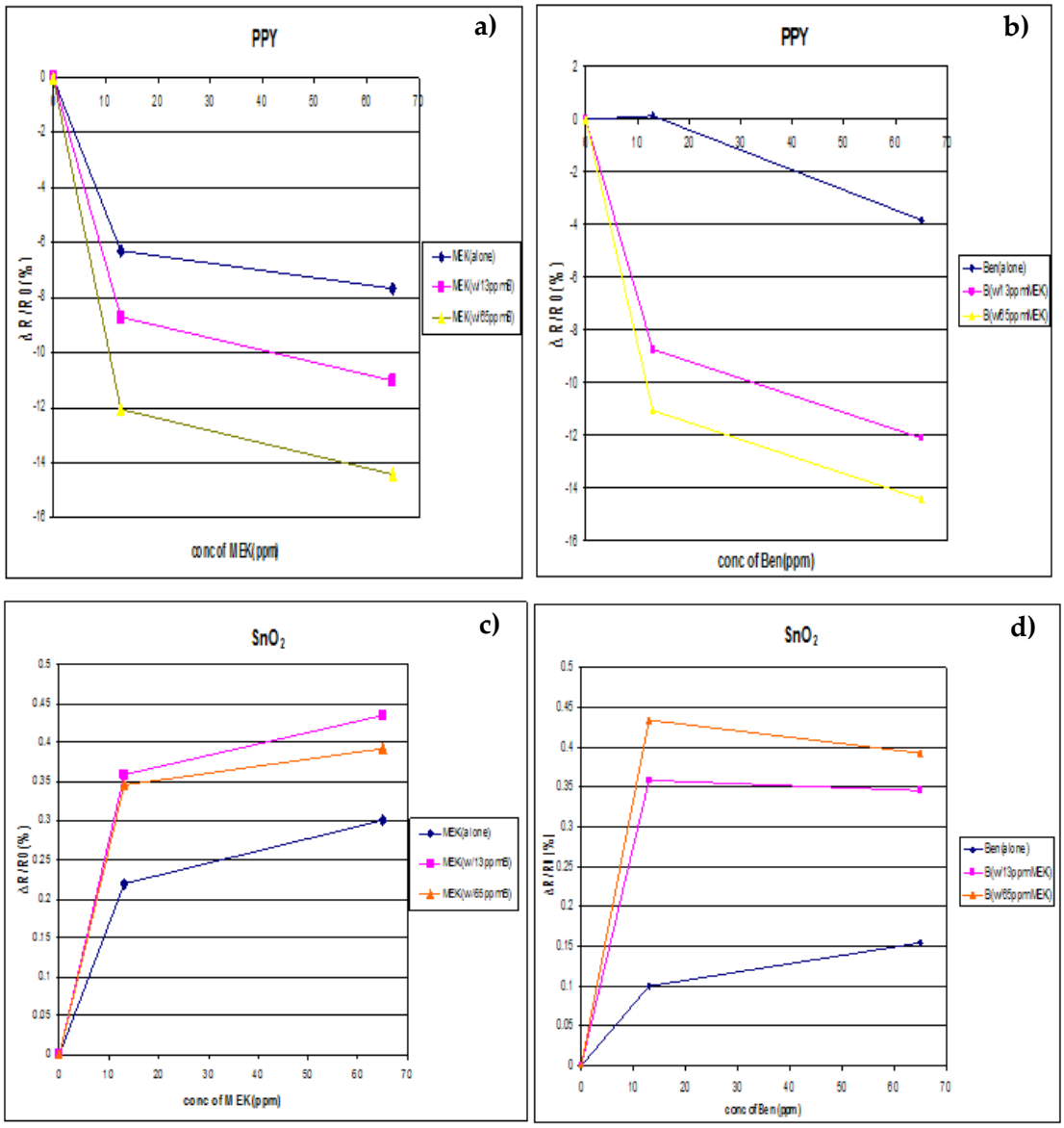

Figure9: Response of SWNT nanosensors functionalized with PPY and SnO_2 to 13 and 65 ppm both benzene and MEK.

4.1.3 Nanosensors arrays to quantify and indentify different VOCs

In this section, an attempt is made to discriminate between MEK and benzene in a mixture of the two analytes in air using a two sensor array. Figure 10 shows that the response relationship of different sensors to different VOCs can be fitted to simple

mathematical models. Here, a Langmuir-like relationship is used which is consistent with the shape of the sensor response and hypothetical sensing mechanism. This was accomplished, although sensing data suffered from having only a limited number of points. Hence, it is possible that sensing characteristics of the sensors were only poorly described, despite excellent fit, with three points only. The "isotherm" or sensor response equation was determined by minimizing the square of the residuals by using trial and error (solver from Excel). As it can seen, the response ($\Delta R/R_0$) the Langmuir-like model appears to give a reasonable trend when applied to the fitting of SnO_2 functionalized SWNT sensors exposed to MEK and benzene. Similarly, a good fit was obtained when PPY functionalized sensors exposed to MEK; a linear model was used for benzene on PPY. Next, it was assumed that the mixture effect is purely addictive, and in this case the response equation for each sensor can be written as

$$R_{PPY} = a*[MEK]/ (1+b*[MEK]) + [Ben]*(_{MEK/ PPY}) \quad (1)$$

$$R_{SnO2} = c*[MEK]/ (1+d*[MEK]) + e*[Ben]/ (1+f* [Ben]) \quad (2)$$

Where, R means the response of a given sensor to the analytes, [analyte] is the concentration of the analyte and m represents the slope of the response of the given sensor upon exposure to the single analyte assuming a linear response. These parameters a through e are constant in the Langmuir equation and are listed in Table 1. Using the best fit values for the responses to individual compounds, the respone equations can be written as:

R_{PPY}= (-2.1402)*[MEK]/ (1+ (0.2643)*[MEK]) + [Ben]*(-0.562) (3)

R_{SnO2}= (0.0499)*[MEK]/ (1+ (0.1510)*[MEK]) + (0.0173)*[Ben]/ (1+ (0.0974)* [Ben]) (4)

Equations 3 and 4 show that, if indeed individual responses are additive, the responses of a two sensor array made e.g., with PPY and SnO_2 should allow to discriminate MEK and benzene, as Equations 3 and 4 form a system of two non-linear equations with only two unknowns, i.e., the concentrations of the two analytes.

Let us take the example of the responses of PPY and SnO_2 functionalized SWNT sensors to benzene and MEK in table 2. Four different mixtures of MEK and benzene were subjected to the above analysis and the predicted concentrations were compared to the actual concentrations. After solving the equations, most the predicted concentrations of benzene are somewhat close to their actual values. However, only one predicted concentrations of MEK is close to its actual value. Thus, this result shows that there is a significant discrepancy between the actual values and the predicted ones. This difference in the results from the individual analyte may result from the non-linearity of the calibration slopes and/or possibly from the non-additivity of the sensor responses. Better calibrations from more concentrations of analytes need to be performed in follow up work. Besides, residuals for the trial and error are mostly on the PPY sensor. This may be related to the fact that the PPY sensor had a lower response to the analytes, hence that a small difference in the PPY response correspond to a large concentration. Another possible reason may be the unstable quality of PPY sensor because of the

oxidation of PPY film after long exposure to air. Oxygen atoms may compete with H atom attached with nitrogen atom on the film surface. This adverse effect may lead to the discrepancy between the predicted and actual value by using PPY functionalized sensors. Even so, the approach illustrated in this example can offer a means to identify and quantify analytes within a mixture after proper calibration, possibly with actual mixtures to discern non-ideal behavior, and proper validation.

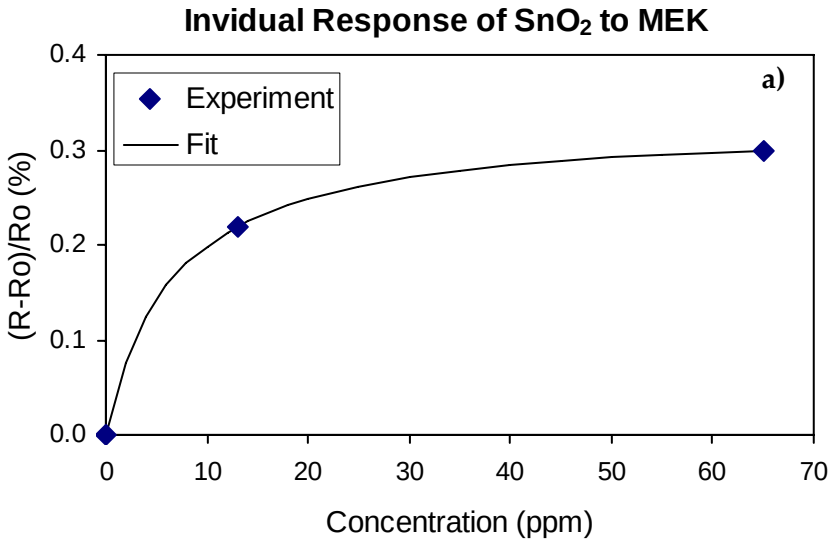

Figure10---Continued

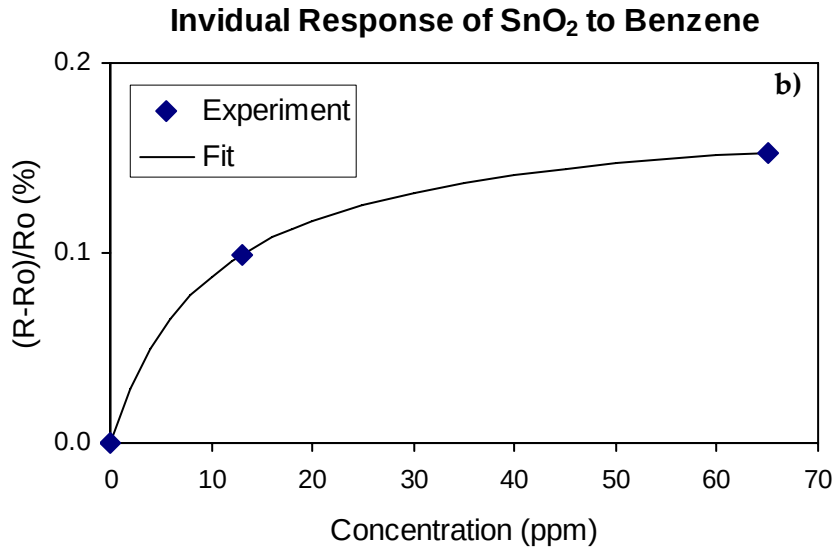

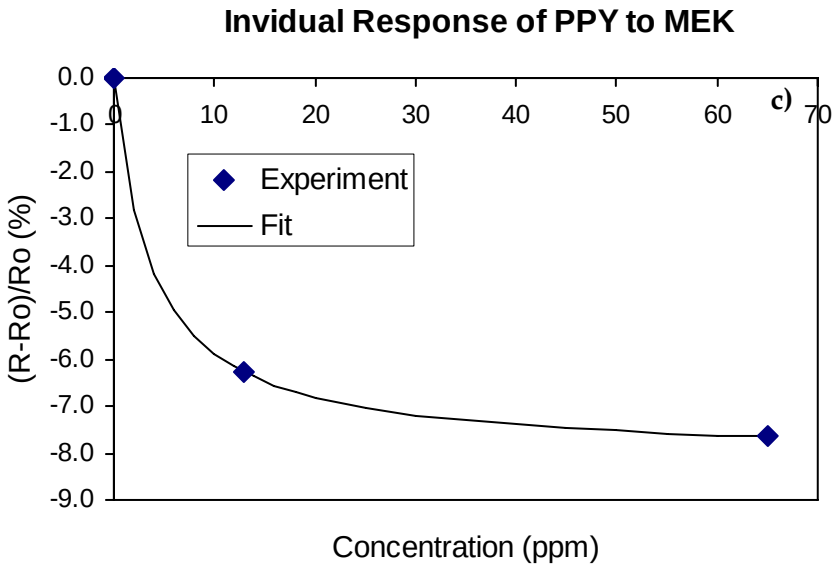

Figure10---Continued

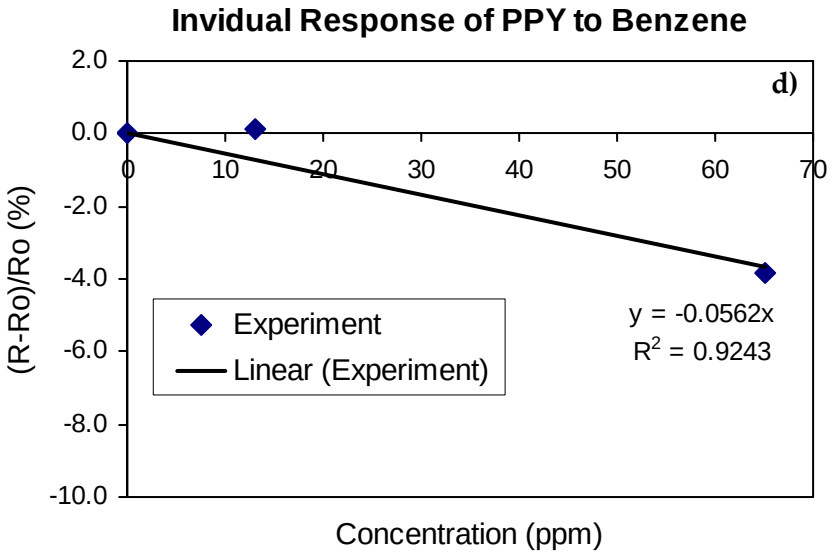

Figure10: Response of SWNT nanosensors functionalized with PPY and SnO_2 to benzene and MEK. A Langmuir-like fit (a~c) and linear fit (d) were taken to model the responses of each sensor to individual analyte.

Table 1: Fitting model characteristics of SWNT nanosensors functionalized with PPY and SnO_2 to individual analytes

Individual Effect	Fit relationship	C_1	C_2
PPY to MEK	Langmuir	a/-2.1402	b/0.2643
PPY to Benzene	Linear	m/-0.0562	
SnO_2 to MEK	Langmuir	c/0.0499	d/0.1510
SnO_2 to Benzene	Langmuir	e/0.0173	f/0.0974

Table 2: Actual analyte value and predicted value by the fitting model and given sensitivity from nanosensors functionalized with PPY and SnO_2 to a mixture of MEK and benzene.

Actual mixture concentrations (ppm)		Measured sensitivity of sensor to the mixture gases		Predicted mixture concentrations (ppm)	
MEK	w/ Benzene	PPY sensor	SnO_2 sensor	MEK w/	Benzene
13	13	-8.721	0.346	177	13
13	65	-12.08	0.358	57	63
65	13	-11.051	0.435	114	7
65	65	-14.424	0.393	54	6

4.2 SEM image of SWNTs coated with Au nanoparticles

Figure 11 shows the SEM images of sensors coated with Au nanoparticles at different deposition charges keeping the electrodeposition potential constant at 0.8V. At lower level of deposition charge (1 μC and 5 μC), relatively few Au particles can be seen on the SWNTs. As deposition charge increases (50 μC and 100 μC), aggregation of Au nanoparticles takes place and Au nanoparticles are more obvious. At the highest level of deposition charge (500 μC), Au nanoparticles are most dense and the largest particle size of all experiments can be seen deposited between the microelectrodes. In addition, the extended deposition of Au nanoparticles may result in the continuous growth of Au forming a film or a wire. The SEM images taken for all decorated samples illustrate that the morphology and size of Au nanoparticles can be regulated by the electrodeposition method by varying the electric deposition charges. As the morphology of the sensors is expected to affect the sensing properties, a series of experiments for mercury sensing

was conducted to define the relationship between deposition charge and electrical conduction in the following sections.

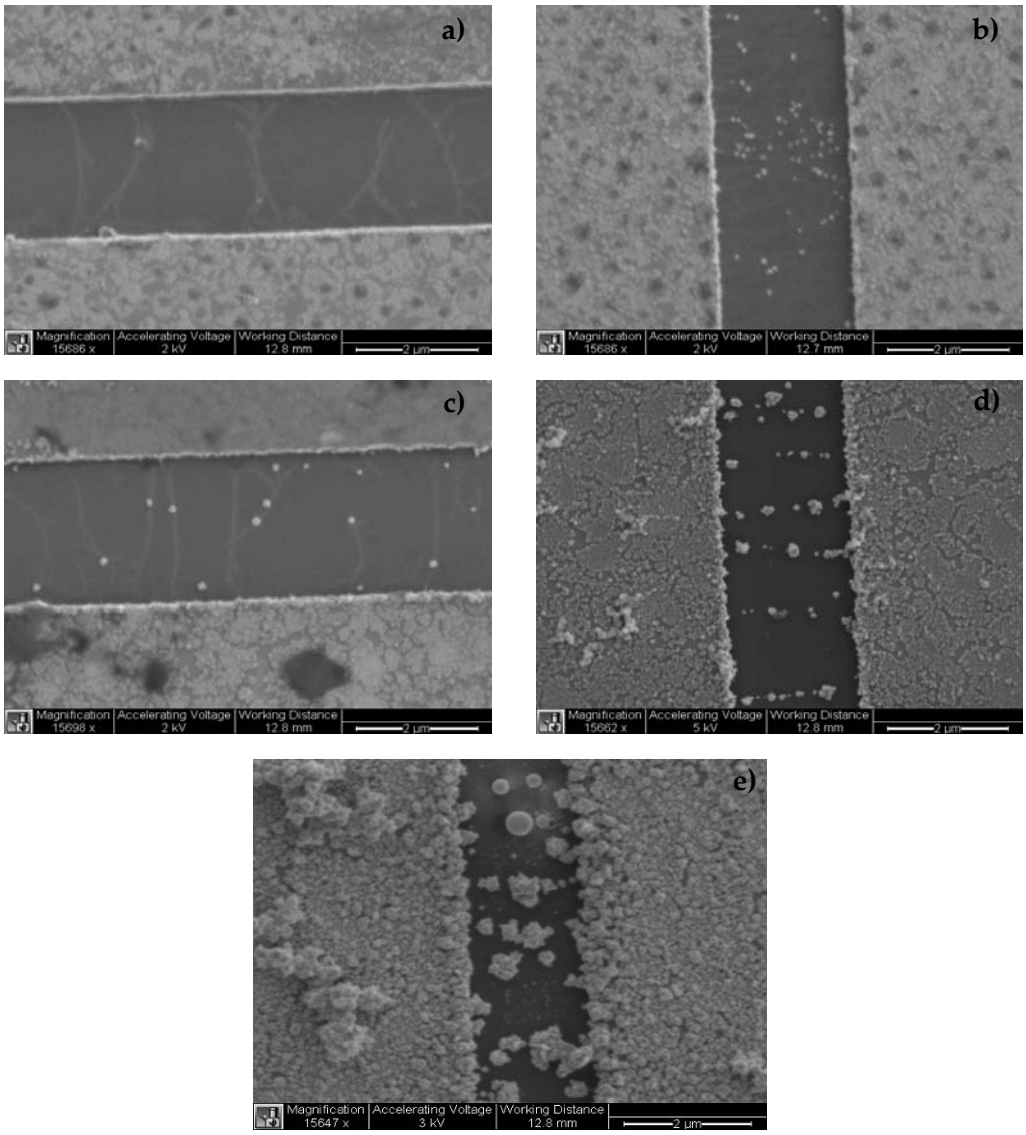

Figure11: SEM image of Au nanoparticles on SWNTs network according to different deposition charges. a): 1µC; b): 5 µC; c): 50 µC; d); 100 µC; e): 500 µC (SEM acquired by Dr. Thomas McNicholas)

4.3 Performance of Au nanoparticle sensor for mercury sensing

4.3.1 Response of Au nanoparticle sensor for mercury vapor

The response of the Au nanoparticle sensor done in our laboratory by Dr. Thomas McNicholas to successive exposures of 2, 5, 10, 30, 50, and 100 ppb at room temperature is shown in Fig 12. After exposure to zero-grade air for around 20 hours to achieve a stable baseline, this sensor has a visible response to mercury vapor in the 2-ppb to 100-ppb range after exposure to mercury vapor. The sensor resistance increased upon exposure to mercury vapor, gradually approaching steady state. After exposure to zero-grade air the resistance of the sensors decreased slowly to ultimately reached the baseline again (see e.g., at 2700 min). When nanosensors were exposed to low concentrations ranging from 2 to 10 ppb, the response of Au nanosensors decorated with low and high deposition charge (5 μC and 100 μC) showed no difference. Both sensors exhibited higher response to 10 ppb mercury than nanosensors decorated with 1 μC. After exposure to low concentrations of mercury, nanosensors decorated with 100 displayed better regeneration at room temperature. Partial regeneration can be observed in nanosensors decorated with 1 μC. No regeneration can bee seen in nanosensors coated with 5 μC. When exposed to high concentrations of mercury ranging from 30 ppb to 100 ppb. A nanosensor coated with 100 μC exhibited better response than nanosensors coated with low deposition charge (1 μC and 5 μC). Saturation was observed at mercury concentration exceeding 100 ppb in a nanosensor decorated with 1

μC. After exposure to high concentrations of mercury, all nanosensors exhibited low regeneration at room temperature. A nanosensor coated with 100 μC may need longer time to show better regeneration at room temperature. The sensor response or sensitivity is defined as $(R-R_0)/R_0$, where R is the steady-state resistance after exposure to mercury vapor and R_0 is the baseline resistance of the sensor in zero-grade air. As shown on Figure 12, the sensitivity had a significant increase with increasing Au deposition. Mercury vapor adsorption relies on the number of Au nanoparticles on SWNTs network. It can be seen that higher density Au nanoparticle sensors exhibit higher magnitude of response. In addition, for the sensor decorated with a high deposition charge (100 μC), there is strong recovery response after exposure even at room temperature. However, the sensor decorated with median density (5 μC) showed relatively weak regeneration. The reasons for the difference were not investigated.

4.3.2 Sensing mechanism of Au nanoparticle sensor

More fundamental work concerning the sensing mechanism of gas nanosensors has been done by others [106, 107, 122]. Previous research has demonstrated that the resistance increase resulting from Hg vapor exposure to Au film. This increasing resistance can be explained by several mechanisms. One research showed that resistance increases may result from the number of conducting electrons. However, this is not applicable because there is a strong interaction between the gas molecules and the surfaces [105]. Another published report showed that the mercury overlayer has a much

shorter mean free path than the initial Au film. Another research presented that the overlayer can be regarded as individual islands of surface assumed to have total diffuse scattering [105]. Various reports converge to suggest that the sensing mechanism for the Au nanosensor is probably due to the formation of Au-Hg amalgam, resulting in an increase in the electrical resistance of the Au-SWNT assembly. Several papers have shown that large adsorbed Hg atoms on Au nanoparticles may lead to the scattering of conduction electron [44, 105-107].

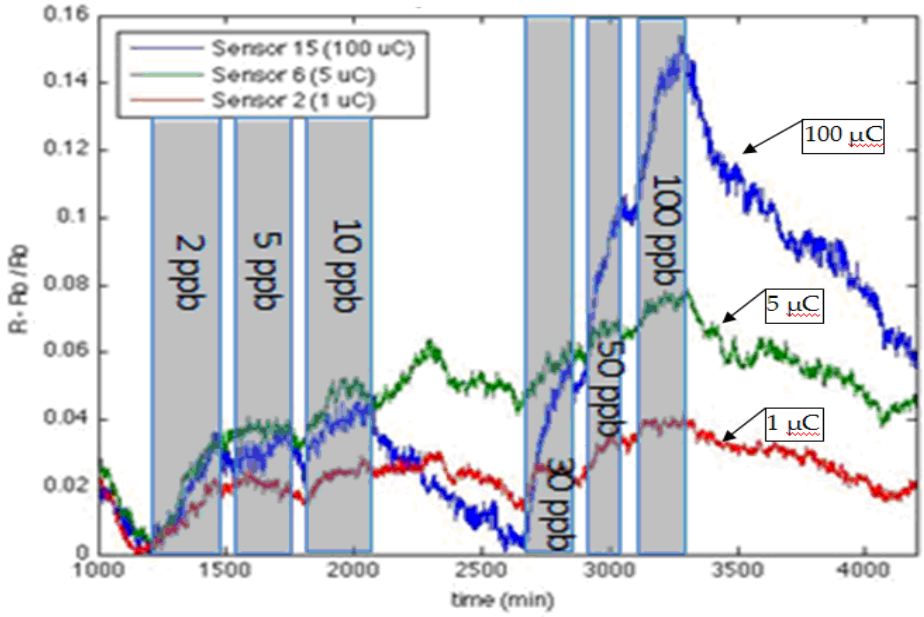

Figure 12: Response of three deposited Au nanoparticle sensors to various concentration of mercury vapor (data acquired by Dr. Thomas McNicholas)

4.3.3 Sensitivity of Au nanoparticle sensor with different deposition charges

As shown in figure 13, the sensitivity plot of $\Delta R/R_0$ shows a somewhat of a linear relationship for concentrations ranging from 2 ppb to 50 ppb, with possible saturation

above 50 ppb for the sensors decorated with different amount of Au nanoparticles. The Au nanosensors coated with 1, 5 and 100 μC respectively showed a linear response 0.02%, 0.09% and 0.13% per ppb Hg. The response of sensors decorated with highest amount is about 6 times higher than that with lowest amount. This result shows that the sensitivity of Au nanosensors is improved by greater amount decorated Au nanoparticles. These results also reveal that the sensitivity can be adjusted by different deposition charges. Additionally, this result also is consistent with previous research [125] and indicates that high-density of Pd nanoparticles on SWNTs result in higher sensitivity to hydrogen.

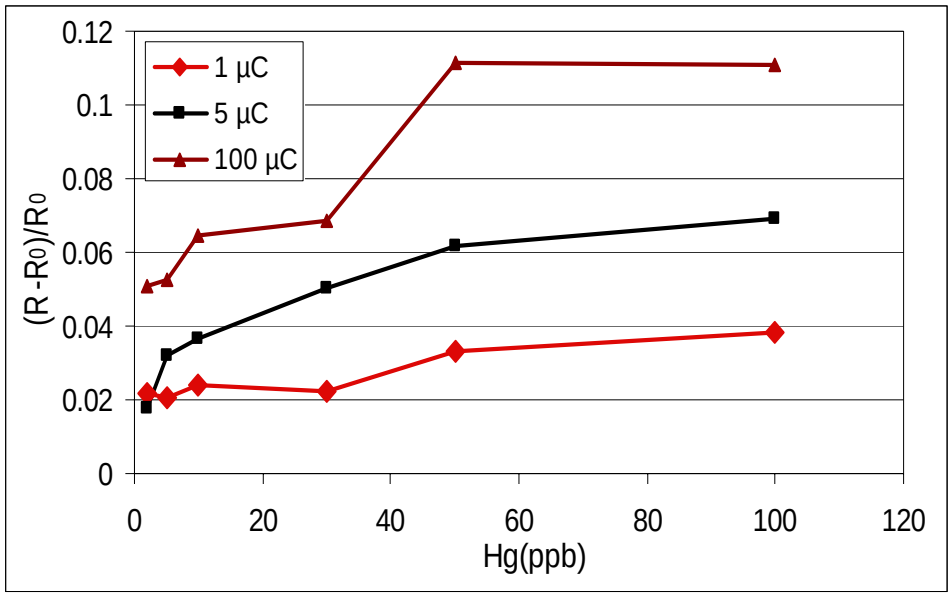

Figure 13: Calibration plots of three deposited Au nanoparticle sensors to various concentrations of vapor mercury (data acquired by Dr. Thomas McNicholas)

A comparison of the responses of mercury sensors reported in the literature to the sensor reported in this study is shown in figure 14. All sensors displayed enhanced

sensitivity to mercury vapor in the ppb range; however, $PdCl_2$ sensors showed no difference in response magnitude above 10 ppb. Among all sensors, Both Au nanosensors with different deposition charges and $PdCl_2$ sensors had the lowest detection limit near 2 ppb. Additionally, Au nanoparticle sensors with 1 μC deposition charge exhibited a response of at least 1.0% per ppb better than $PdCl_2$ sensors, which was near 0.6 % per ppb mercury vapor. At room temperature, polymer composite sensors showed regeneration time within 1 hour, which is much shorter than our Au nanoparticles sensors which required close to 15 hours. However, lower regeneration can be observed when $PdCl_2$ sensors are exposed to mercury vapor and no regeneration of the abraded gold film sensors are found. In all cases, it appears that each type of sensor can have repeatable responses, thus displaying good reproducibility of response at ppb concentrations levels. In summary, Au nanoparticles sensor exhibited higher sensitivity and reproducibility as well as had a lower detection limit; it can also be expected that this sensor could be more cost-effective compared to other sensors because of the simple manufacturing techniques [106, 107]. The major drawback of abraded gold film sensors is lack of regeneration at room temperature. Research has shown that regeneration would be improved at high temperature [105, 107]. As for $PdCl_2$ sensors, the restrictions of narrow working temperature are important [107, 109]. Higher temperature may decrease the regeneration time; however, may lead to both the leakage of substrate material and the lower sensitivity. The polymer-carbon composite sensors

have been broadly responsive to various analytes, are easily fabricated, benefit from strong regeneration and are cost effective; nevertheless, the detection limit of this sensor may not be low enough to meet the requirement of 3 ppb, for toxicological studies or NASA's need in spacecraft.

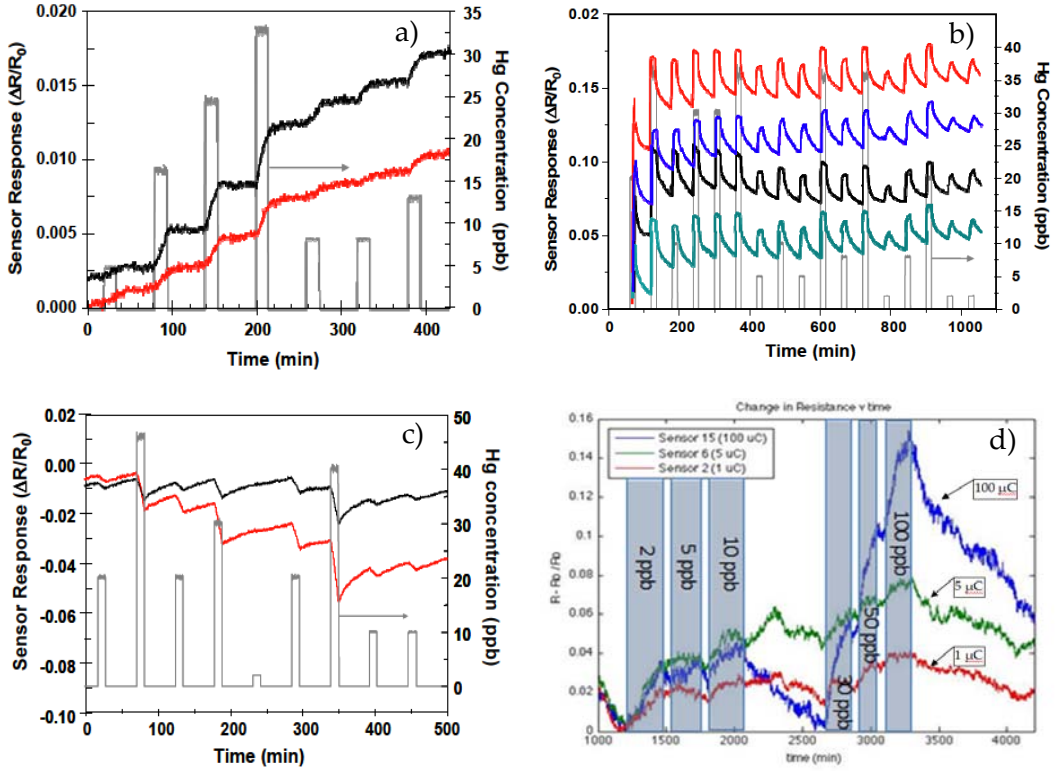

Figure 14: Comparison of the responses of previous mercury vapor. a): Abraded gold film sensors [107]; b): $PdCl_2$ sensors [107]; c): Polymer-carbon composite sensors [107]; d): Au nanoparticle sensors ([107], d) Au nanoparticle sensors (same as Figure 12)

5. Conclusions and future work

PPY and SnO_2 functionalized SWNT sensors were shown to be broadly sensitive to VOCs including xylene, MEK, hexane and benzene. Compared to current sensors, these nanoscale sensors showed a medium response time and higher sensitivity to low concentration of analytes at room temperature. This result indicates nanosensors have area high affinity to low concentrations of the target VOCs. SnO_2 films may exhibit polar interactions with the adsorbate, resulting in higher sensitivity to MEK. Additionally, swelling and adsorption effects could have occurred between PPY and some of the analytes contributing to the sensing response. Hexane and xylene absorption into PPY films may increase the distance between PPY molecules, resulting higher electrical resistance. However, increasing conductivity of the PPY sensor to xylene and hexane was also observed. The details of the exact sensing mechanisms are not clear. A non-linear and additive sensor response approach was used in an attempt to discriminate between MEK and benzene in a mixture, but a large difference was observed between predicted and actual concentrations when nanosensors upon exposure to MEK. PPY sensor may contribute to this discrepancy because of interfere of oxygen atoms attracting hydrogen atom attached on nitrogen atom. Further refinement of the method is needed before one is capable of discriminating mixtures of volatile with arrays of functionalize SWNT sensors. Even so, the result indicates that sensor arrays can be good

candidates for identifying analytes in mixtures, especially for polar and nonpolar compounds.

The responses of mercury vapor and VOC nanosensors have been presented and discussed. The sensor was fabricated at UCR by electrodepositing Au nanoparticles on SWNTs and tested at Duke. The sensors were found to be able to detect 3 ppb of mercury vapor in air at room temperature. The results showed that high sensing sensitivity result from high deposition charge of Au nanoparticles on SWNTs networks. The Au-SWNT sensors further showed excellent regeneration and reproducibility compared to current mercury sensors. In comparison, gold film sensors, $PdCl_2$ and SAW-based sensors all require elevated temperatures for regeneration. Polymer-carbon composite sensors have been shown to respond reproducibly to vapor concentration from 10 to 45 ppb, and have good regeneration capability at room temperature. However, their detection limit may not meet the requirements for either occupational health or NASA's needs.

Future work on these sensors should focus on several aspects. SWNTs with PPY and SnO_2 sensors need an improvement in reproducibility. Short reaction and recovery time are desired to make Au-SWNT sensors more robust and useable in different environments. Advanced fabrication technology should address these problems by inventing new platform to offer e.g., high temperature to increase recovery rate and decrease response time. Furthermore, the sensing mechanism of PPY and SnO_2 sensors

to polar and nonpolar VOCs should be investigated by a variety of tools such as Atomic Force Microscope and X-ray Photoemission Spectrometer, to understand the interaction of analytes and sensing materials' surfaces. This work can help researchers make suitable sensor arrays that will ultimately allow to identify and quantify various compounds including VOCs and greenhouse gases by using PPY and SnO_2 sensors.

References

1. Ciganek, M. and J. Neca, *Chemical characterization of volatile organic compounds on animal farms.* VETERINARNI MEDICINA, 2008. **53**(12): p. 641-651

2. Schiffman, S.S., J.L. Bennett, and J.H. Raymer, *Quantification of odors and odorants from swine operations in North Carolina.* AGRICULTURAL AND FOREST METEOROLOGY, 2001. **108**(3): p. 213-240.

3. Lee, C.S., F. Haghighat, and W.S. Ghaly, *A study on VOC source and sink behavior in porous building materials - analytical model development and assessment.* Indoor Air, 2005. **15**(3): p. 183-96.

4. U.S. DEPARTMENT OF LABOR , *Permissible Exposure Limits*[on-line webpage].URL: http://www.osha.gov/SLTC/pel/

5. Lin, C.W., S.S. Liu, and B.J. Hwang, *Study of the actions of BTEX compounds on polypyrrole film as a gas sensor.* Journal of Applied Polymer Science, 2001. **82**(4): p. 954-961.

6. Rowe, B.L., et al., *Occurrence and potential human-health relevance of volatile organic compounds in drinking water from domestic wells in the United States.* Environmental Health Perspectives, 2007. **115**(11): p. 1539-1546

7. Lim, C.B., et al., *Sensing characteristics of nano-network structure of polypyrrole for volatile organic compounds (VOCs) gases.* 2006 IEEE SENSORS, VOLS 1-3, 2006: p. 710-713.

8. United Nations Environmental Program, *Water on Tap-what you need to know* [on-line webpage]. URL: http://www.epa.gov/safewater/wot/pdfs/book_waterontap_full.pdf

9. United Nations Environmental Program, *Drinking Water Contaminants* [on-line webpage]. URL: http://www.epa.gov/safewater/contaminants/index.html

10. Jun, H.K., et al., *Electrical properties of polypyrrole gas sensors fabricated under various pretreatment conditions.* Sensors and Actuators B-Chemical, 2003. **96**(3): p. 576-581.

11. Lonergan, M.C., et al., Array-based vapor sensing using chemically sensitive, carbon black-polymer resistors. Chemistry of Materials, 1996. **8**(9): p. 2298-2312

12. Horrillo, M.C., et al., *Measurements of VOCs with a semiconductor electronic nose.* Journal of the Electrochemical Society, 1998. **145**(7): p. 2486-2489

13. Bo, L., et al., *Volatile Organic Compound Detection Using Nanostructured Copolymers.* Nano Letters, 2006. **6**(8): p. 1598-1602.

14. Srivastava, A.K., *Detection of volatile organic compounds (VOCs) using SnO_2 gas-sensor array and artificial neural network.* Sensors and Actuators B-Chemical, 2003. **96**(1-2): p. 24-37

15. Nayak, M.S., R. Dwivedi, and S.K. Srivastava, *SENSITIVITY AND RESPONSE-TIMES OF DOPED TIN OXIDE INTEGRATED GAS SENSORS.* Microelectronics Journal, 1994. **25**(1): p. 17-25

16. Yamada, Y., et al., *A semiconductor gas sensor system for high throughput screening of heterogeneous catalysts for the production of benzene derivatives.* MEASUREMENT SCIENCE & TECHNOLOGY, 2005. **16**(1): p. 229-234.

17. Deng, Z.P., D.C. Stone, and M. Thompson, *Characterization of polymer films of pyrrole derivatives for chemical sensing by cyclic voltammetry, X-ray photoelectron spectroscopy and vapour sorption studies.* ANALYST, 1997. **122**(10): p. 1129-1138

18. Hamilton, S., M.J. Hepher, and J. Sommerville, *Polypyrrole materials for detection and discrimination of volatile organic compounds.* Sensors & Actuators B: Chemical, 2005. **107**(1): p. 424-432.

19. Seinfeld, J.H., *Atmospheric chemistry and physics of air pollution*. Air pollution: New York : Wiley, c1986

20. Gajdosik, L., The concentration measurement with SnO_2 gas sensor operated in the dynamic regime. Sensors and Actuators B-Chemical, 2005. 106(2): p. 691-699

21. Meixner, H. and U. Lampe, *Metal oxide sensors.* Sensors and Actuators B: Chemical, 1996. **33**(1-3): p. 198-202.

22. Tomchenko, A.A., et al., *Semiconducting metal oxide sensor array for the selective detection of combustion gases.* Sensors & Actuators B: Chemical, 2003. **93**(1-3): p. 126

23. Schwarzenbach, R.P., *Environmental organic chemistry*, ed. P.M. Gschwend and D.M. Imboden: Hoboken, N.J. : Wiley, c2003.

24. Persaud, K.C., et al., *Sensor array techniques for mimicking the mammalian olfactory system.* Sensors and Actuators B: Chemical, 1996. **36**(1-3): p. 267-273

25. Yadong, J., et al., *Study on the NH3-gas sensitive properties and sensitive mechanism of polypyrrole.* Sensors and Actuators B: Chemical, 2000. **66**(1-3): p. 280-282

26. Penza, M., et al., *AC and DC measurements on Langmuir-Blodgett polypyrrole films for selective NH3 gas detection.* MATERIALS SCIENCE & ENGINEERING C-BIOMIMETIC MATERIALS SENSORS AND SYSTEMS, 1998. **5**(3-4): p. 255-258.

27. Lee, Y.-S., et al., *Visible optical sensing of ammonia based on polyaniline film.* Sensors & Actuators B: Chemical, 2003. **93**(1-3): p. 148

28. Giorgio, Sberveglieri., *Gas Sensor: Priciples, operation, and development.* 1992, New York: Springer-Verlag. 424 p

29. Counter, S.A. and L.H. Buchanan, *Mercury exposure in children - a review*. Toxicology and Applied Pharmacology, 2004. **198**(2): p. 209-230.

30. Nriagu, J.O., *A global assessment of natural sources of atmospheric trace metals.* Nature, 1989. **338**(2): p. 47-49.

31. Pirrone, N., et al., *Global mercury emissions to the atmosphere from anthropogenic and natural sources.* Atmospheric Chemistry and Physics Discussions, 2010. **10**(2): p. 4719-4752

32. Carpi, A., *Mercury from combustion sources: A review of the chemical species emitted and their transport in the atmosphere.* Water Air and Soil Pollution, 1997. **98**(3-4): p. 241-254.

33. Streets, D.G., et al., *Anthropogenic mercury emissions in China.* Atmospheric Environment, 2005. **39**(40): p. 7789-7806

34. Slemr, F. and E. Langer, *Increase in global atmospheric concentrations of mercury inferred from measurements over the Atlantic Ocean*. Nature, 1992. **355**(30): p. 434-437

35. Pirrone, N., et al., *Modeling mercury emissions from forest fires in the Mediterranean region.* Environmental Fluid Mechanics, 2008. **8**(2): p. 129-145

36. Mason, R.P., *Mercury Emissions from Natural Process and their importance in the Global Mercury Cyclety.* 2009, New York: Springer. 173 p

37. United Nations Environmental Program, *Mercury pollution - transport and cycle* [on-line webpage]. URL: http://maps.grida.no/go/graphic/mercury_pollution_transport_and_cycle.

38. Pirrone, N., et al., *Dynamic process of mercury over the Mediterranean region: results from the Mediterranean Atomospheric Mercury Cycle System (MAMCS) project, Dynamic process of mercury and other trace contaminants in the marine boundary layer of European seas - ELOISE II.* Atomospheric Environment, 2003. **37**(1): p. 109-117

39. Pirrone, N., et al., *MDynamic Processes of Atmospheric Hg in the Mediterranean Region.* 2005, New York: Springer. 541 p.

40. Hedgecock, I.M., et al., *Integrated mercury cycling, transport, and air-water exchange (MECAWEx) model.* J. Geophys. Res., 2006. **111**(D20): p. D20302

41. Wang, Q., W.G. Shen, and Z.W. Ma, *Estimation of mercury emission from coal combustion in China.* Environmental Science & Technology, 2000. **34**(13): p. 2711-2713.

42. Zahir, F., et al., *Low dose mercury toxicity and human health.* Environmental Toxicology and Pharmacology, 2005. **20**(2): p. 351-360

43. Chu, P. and D.B. Porcella, *Mercury Stack Emissions from Us Electric Utility Power-Plants.* Water Air and Soil Pollution, 1995. **80**(1-4): p. 135-144

44. Keebaugh, S., et al., *Gold nanowires for the detection of elemental and ionic mercury.* Electrochemical and Solid State Letters, 2006. **9**(9): p. H88-H91.

45. Pirrone, N., et al., *Global Mercury Emissions to the Atmosphere form Natural and Anthropogenic Sources.* 2009, New York: Springer. 3 p.

46. Qi, X., et al., *An evaluatioin of mercury emissions from the chlor-alkali industry in China.* Journal of Environmental Sources, 2000. **12**: p. 24-30.

47. Feng, X.B., G.H. Li, and G.L. Qiu, *A preliminary study on mercury contamination to the environment from artisanal zinc smelting using indigenous methods in Hezhang County, Guizhou, China: Part 2. Mercury contaminations to soil and crop.* Science of the Total Environment, 2006. **368**(1): p. 47-55

48. U.S. ENVIRONMENTAL PROTECTION AGENCY, *Mercury Study Report to Congress (December 1997)* [on-line webpage].URL: http://www.epa.gov/ttn/oarpg /t3/reports/volume2.pdf.

49. U. S. Energy Information Administration, *International Energy Outlook (May 2009)* [on-line webpage].URL: http://www.eia.doe.gov/oiaf/ieo/pdf/0484(2009).pdf.

50. Feng, X., et al., *Mercury emissions from industrial sources in China.* 2009, New York: Springer. 67 p.

51. Slemr, F., G. Schuster, and W. Seiler, *Distribution, Speciation, and Budget of Atmospheric Mercury.* Journal of Atmospheric Chemistry, 1985. **3**(4): p. 407-434

52. Lindqvist, O. and H. Rodhe, *Atmospheric Mercury - a Review.* Tellus Series B-Chemical and Physical Meteorology, 1985. **37**(3): p. 136-159

53. Schroeder, W., G. Yarwood, and H. Niki, *Transformation processes involving mercury species in the atmosphere — results from a literature survey.* Water, Air, & Soil Pollution, 1991. **56**(1): p. 653-666

54. Brosset, C., *The behavior of mercury in the physical environment.* Water, Air, & Soil Pollution, 1987. **34**(2): p. 145-166

55. Brosset, C. and E. Lord, *Mercury in precipitation and ambient air a new scenario.* Water, Air, & Soil Pollution, 1991. **56**(1): p. 493-506

56. Schroeder, W., G. Yarwood, and H. Niki, *Transformation processes involving mercury species in the atmosphere — results from a literature survey.* Water, Air, & Soil Pollution, 1991. **56**(1): p. 653-666.

57. Meit, R., *The fate of mercury in coal-fired power plants and the influence of wet flue-gas desulphurization.* Water, Air, & Soil Pollution, 1991. **56**(1): p. 21-33

58. Hall, B., P. Schager, and O. Lindqvist, *Chemical reactions of mercury in combustion flue gases.* Water, Air, & Soil Pollution, 1991. **56**(1): p. 3-14.

59. Iverfeldt, Å., *Mercury in forest canopy throughfall water and its relation to atmospheric deposition.* Water, Air, & Soil Pollution, 1991. **56**(1): p. 553-564.

60. Munthe, J., *The Aqueous Oxidation of Elemental Mercury by Ozone.* Atmospheric Environment Part a-General Topics, 1992. **26**(8): p. 1461-1468

61. Munthe, J., Z.F. Xiao, and O. Lindqvist, *The aqueous reduction of divalent mercury by sulfite.* Water, Air, & Soil Pollution, 1991. **56**(1): p. 621-630

62. Coelho-Souza, S.A., et al., *Mercury methylation and bacterial activity associated to tropical phytoplankton.* Science of the Total Environment, 2006. **364**(1-3): p. 188-199.

63. Gilbert, S.G. and K.S. Grantwebster, *Neurobehavioral Effects of Developmental Methylmercury Exposure.* Environmental Health Perspectives, 1995. **103**: p. 135-142

64. Chadhain, S.M.N., et al., *Analysis of mercuric reductase (merA) gene diversity in an anaerobic mercury-contaminated sediment enrichment.* Environmental Microbiology, 2006. **8**(10): p. 1746-1752.

65. Barkay, T., S.M. Miller, and A.O. Summers, *Bacterial mercury resistance from atoms to ecosystems.* Fems Microbiology Reviews, 2003. **27**(2-3): p. 355-384

66. Barkay, T. and I. Wagner-Dobler, *Microbial transformations of mercury: Potentials, challenges, and achievements in controlling mercury toxicity in the environment.* Advances in Applied Microbiology, Vol 57, 2005. **57**: p. 1-52

67. Compeau, G.C. and R. Bartha, *Sulfate-Reducing Bacteria: Principal Methylators of Mercury in Anoxic Estuarine Sediment.* Appl. Environ. Microbiol., 1985. **50**(2): p. 498-502.

68. Devereux, R., et al., *Depth profile of sulfate-reducing bacterial ribosomal RNA and mercury methylation in an estuarine sediment.* Fems Microbiology Ecology, 1996. **20**(1): p. 23-31

69. Benoit, J.M., C.C. Gilmour, and R.P. Mason, *Aspects of Bioavailability of Mercury for Methylation in Pure Cultures of Desulfobulbus propionicus (1pr3).* Appl. Environ. Microbiol., 2001. **67**(1): p. 51-58

70. King, J.K., et al., *Sulfate-Reducing Bacteria Methylate Mercury at Variable Rates in Pure Culture and in Marine Sediments.* Appl. Environ. Microbiol., 2000. **66**(6): p. 2430-2437

71. King, J.K., et al., *A quantitative relationship that remonstrates mercury methylation rates in marine sediments are based on the community composition and activity of sulfate-reducing bacteria.* Environmental Science & Technology, 2001. **35**(12): p. 2491-2496

72. King, J.K., et al., *Mercury removal, methylmercury formation, and sulfate-reducing bacteria profiles in wetland mesocosms.* Chemosphere, 2002. **46**(6): p. 859-70.

73. Balogh, S.J., et al., *Episodes of elevated methylmercury concentrations in prairie streams.* Environmental Science & Technology, 2002. **36**(8): p. 1665-1670.

74. Bloom, N.S., *On the Chemical Form of Mercury in Edible Fish and Marine Invertebrate Tissue.* Canadian Journal of Fisheries and Aquatic Sciences, 1992. **49**(5): p. 1010-1017

75. Hall, B.D., et al., *Food as the dominant pathway of methylmercury uptake by fish.* Water Air and Soil Pollution, 1997. **100**(1-2): p. 13-24

76. Hansen, J.C. and G. Danscher, *Organic mercury: an environmental threat to the health of dietary-exposed societies?* Rev Environ Health, 1997. **12**(2): p. 107-16

77. Satoh, H., *Occupational and environmental toxicology of mercury and its compounds.* Industrial Health, 2000. **38**(2): p. 153-164

78. Goldwater, L.J., *The Toxicology of Inorganic Mercury.* Annals of the New York Academy of Sciences, 1957. **65**(5): p. 498-503

79. Malm, O., *Gold mining as a source of mercury exposure in the Brazilian Amazon.* Environmental Research, 1998. **77**(2): p. 73-78

80. Ratcliffe, H.E., G.M. Swanson, and L.J. Fischer, *Human exposure to mercury: A critical assessment of the evidence of adverse health effects.* Journal of Toxicology and Environmental Health, 1996. **49**(3): p. 221-270

81. Sweet, L.I. and J.T. Zelikoff, *Toxicology and immunotoxicology of mercury: A comparative review in fish and humans.* Journal of Toxicology and Environmental Health-Part B-Critical Reviews, 2001. **4**(2): p. 161-205

82. Vroom, F.Q. and M. Greer, *Mercury Vapor Intoxication.* Environmental Health, 1996. **49**(3): p. 221-270

83. Williams, J.E. and C.F. Schram, *Acute mercurial poisoning*. Ind. Med., 1937.**6**(): p. 490-491

84. United States. Agency for Toxic Substances and Disease Registry., *Agency profile and annual report*. 1992, The Agency: Atlanta, Ga. p. v

85. Campbell, J.S., *Acute mercurial poisoning by inhalation of metallic vapour in an infant.* Canadian Medical Association Journal, 1948. **58**(1): p. 72-5

86. Matthes, F.T., et al., *Acute poisoning associated with inhalation of mercury vapor; report of four cases.* Pediatrics, 1958. **22**(4 Part 1): p. 675-88

87. Moutinho, M.E., et al., *Acute mercury vapor poisoning. Fatality in an infant.* Am J Dis Child, 1981. **135**(1): p. 42-4

88. Samuels, E.R., et al., *A case of accidental inorganic mercury poisoning.* J Anal Toxicol, 1982. **6**(3): p. 120-2

89. *Public health assessments completed. Agency for Toxic Substances and Disease Registry (ATSDR), Department of Health and Human Services (HHS). Notice.* Fed Regist, 1999. **64**(18): p. 4422-3

90. Halbach, S. and T.W. Clarkson, *Enzymatic Oxidation of Mercury-Vapor by Erythrocytes.* Biochimica Et Biophysica Acta, 1978. **523**(2): p. 522-531

91. Hussain, S., et al., *Mercuric chloride-induced reactive oxygen species and its effect on antioxidant enzymes in different regions of rat brain.* Journal of Environmental Science and Health Part B-Pesticides Food Contaminants and Agricultural Wastes, 1997. **32**(3): p. 395-409

92. Dieguez-Acuna, F.J., et al., *Nuclear Factor {kappa}B Activity Determines the Sensitivity of Kidney Epithelial Cells to Apoptosis: Implications for Mercury-Induced Renal Failure.* Toxicol. Sci., 2004. **82**(1): p. 114-123

93. Ellingsen, D.G., et al., *Renal and immunologic markers for chloralkali workers with low exposure to mercury vapor.* Scandinavian Journal of Work Environment & Health, 2000. **26**(5): p. 427-435

94. Aberg, B., et al., *Metabolism of Methyl Mercury (203hg) Compounds in Man - Excretion and Distribution.* Archives of Environmental Health, 1969. **19**(4): p. 478-&

95. Dabeka, R., et al., *Survey of total mercury in some edible fish and shellfish species collected in Canada in 2002.* Food Additives and Contaminants, 2004. **21**(5): p. 434-440

96. Schuhmacher, M., et al., *Mercury Concentrations in Marine Species from the Coastal Area of Tarragona Province, Spain - Dietary-Intake of Mercury through Fish and Seafood Consumption.* Science of the Total Environment, 1994. **156**(3): p. 269-273

97. Duffy, L.K., T. Rodgers, and M. Patton, *Regional health assessment relating to mercury content of fish caught in the Yukon-Kuskokwim Delta rivers system.* Alaska Med, 1998. **40**(4): p. 75-7, 89

98. Palheta, D. and A. Taylor, *Mercury in Environmental and Biological Samples from a Gold Mining Area in the Amazon Region of Brazil.* Science of the Total Environment, 1995. **168**(1): p. 63-69

99. Hirayama, K., *Effects of Combined Administration of Thiol Compounds and Methylmercury Chloride on Mercury Distribution in Rats.* Biochemical Pharmacology, 1985. **34**(11): p. 2030-2032

100. Thomas, D.J. and J.C. Smith, *Effects of Co-Administered Low-Molecular-Weight Thiol Compounds on Short-Term Distribution of Methyl Mercury in the Rat.* Toxicology and Applied Pharmacology, 1982. **62**(1): p. 104-110

101. Sager, P.R., R.A. Doherty, and P.M. Rodier, *Effects of Methylmercury on Developing Mouse Cerebellar Cortex.* Experimental Neurology, 1982. **77**(1): p. 179-193

102. Castoldi, A.F., et al., *Neurotoxicity and molecular effects of methylmercury.* Brain Res Bull, 2001. **55**(2): p. 197-203

103. Clarkson, T.W., *Mercury: major issues in environmental health.* Environ Health Perspect, 1993. **100**: p. 31-8

104. *World Health Organization. WHO publications.* 1990. *Geneva*

105. Mcnerney, J.J., R.C. Hanson, and P.R. Buseck, *Mercury Detection by Means of Thin Gold Films.* Science, 1972. **178**(4061): p. 611-&

106. Caron, J.J., et al., *Surface acoustic wave mercury vapor sensor.* Ieee Transactions on Ultrasonics Ferroelectrics and Frequency Control, 1998. **45**(5): p. 1393-1398

107. Shevade, A.V., et al., *Developement of the third genenration JPL electronic nose for international space station technology demonstration.* SAE International, 2007. **1**: p. 3149-315

108. Selid, P.D., et al., *Sensing Mercury for Biomedical and Environmental Monitoring.* Sensors, 2009. **9**(7): p. 5446-5459

109. Ruys, D.P., J.F. Andrade, and O.M. Guimaraes, *Mercury detection in air using a coated piezoelectric sensor.* Analytica Chimica Acta, 2000. **404**(1): p. 95-100

110. Keller, L.O., et al., *Towards Nano-Fin based Mercury-Sensors.* 2009: p. 342-344

111. Durkan, C. and M.E. Welland, *Size effects in the electrical resistivity of polycrystalline nanowires.* Physical Review B, 2000. **61**(20): p. 14215-14218

112. Severin, E.J. and N.S. Lewis, *Relationships among resonant frequency changes on a coated quartz crystal microbalance, thickness changes, and resistance responses of polymer-carbon black composite chemiresistors.* Analytical Chemistry, 2000. **72**(9): p. 2008-2015

113. Lonergan, M.C., et al., Array-based vapor sensing using chemically sensitive, carbon black-polymer resistors. Chemistry of Materials, 1996. **8**(9): p. 2298-2312

114. Rufer, L., et al., *GaAs and GaN based SAW chemical sensors: acoustic part design and technology.* 2006: p. 165-168

115. Carlen, E.T. and A. van den Berg, *Nanowire electrochemical sensors: can we live without labels?* Lab on a Chip, 2007. **7**(1): p. 19-23

116. Kauffman, D.R., et al., *Understanding the Sensor Response of Metal-Decorated Carbon Nanotubes.* Nano Letters, 2010. **10**(3): p. 958-963

117. Ryan, M.A., et al., *Polymer-carbon black composite sensors in an electronic nose for air-quality monitoring.* Mrs Bulletin, 2004. **29**(10): p. 714-719

118. Murphy, P.J., *Determination of Nanogram Quantities of Mercury in Liquid Matrices by a Gold Film Mercury Detector.* Analytical Chemistry, 1979. **51**(9): p. 1599-1600

119. Ryan, M.A., et al., *Conductometric Sensors for Detection of Elemental Mercury Vapor.* ECS Transactions, 2008. **16**(11): p. 431-439

120. Cui, Y., et al., *Nanowire nanosensors for highly sensitive and selective detection of biological and chemical species.* Science, 2001. **293**(5533): p. 1289-1292

121. Severin, E.J. and N.S. Lewis, *Relationships among resonant frequency changes on a coated quartz crystal microbalance, thickness changes, and resistance responses of polymer-carbon black composite chemiresistors.* Analytical Chemistry, 2000. **72**(9): p. 2008-2015

122. Lonergan, M.C., et al., Array-based vapor sensing using chemically sensitive, carbon black-polymer resistors. Chemistry of Materials, 1996. **8**(9): p. 2298-2312

123. Lim, C.B., et al., *Sensing characteristics of nano-network structure of polypyrrole for volatile organic compounds (VOCs) gases.* 2006 IEEE SENSORS, VOLS 1-3, 2006: p. 710-713

124. Hernandez, S.C., et al., *Single polypyrrole nanowire ammonia gas sensor.* Electroanalysis, 2007. **19**(19-20): p. 2125-2130

125. Mubeen, S., et al., *Palladium Nanoparticles Decorated Single-Walled Carbon Nanotube Hydrogen Sensor.* The Journal of Physical Chemistry C, 2007. **111**(17): p. 6321-6327

126. Mubeen, S., et al., *Sensitive Detection of H2S Using Gold Nanoparticle Decorated Single-Walled Carbon Nanotubes.* Analytical Chemistry, 2009. **82**(1): p. 250-257

127. Mubeen, S., et al., *Hybrid Metal Oxide-SWNT Nanostructures based Gas Sensor. In Press*

128. Mubeen, S., et al., *Sensitive Detection of H2S Using Gold Nanoparticle Decorated Single-Walled Carbon Nanotubes.* Analytical Chemistry, 2009. **82**(1): p. 250-258

129. Lee, C.Y. and M.S. Strano, *Amine Basicity (pKb) Controls the Analyte Binding Energy on Single Walled Carbon Nanotube Electronic Sensor Arrays.* Journal of the American Chemical Society, 2008. **130**(5): p. 1766-1773

130. Giorgio, Sberveglieri., *Gas Sensor: Priciples, operation, and development.* 1992, New York: Springer-Verlag. 424 p